A STUDY OF U(1) LATTICE GAUGE THEORY IN FOUR DIMENSIONS

by

Christodoulos NIKOLAKIS-MOUHAS

Thesis submitted for the degree of Doctor of Philosophy of the University of London.

Royal Holloway College, 1985

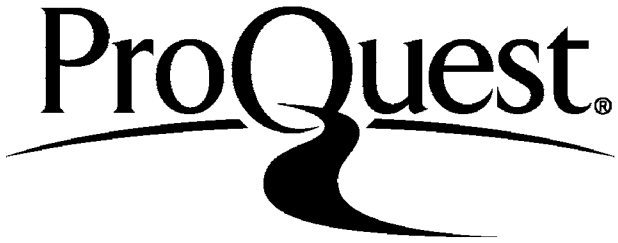

A STUDY OF U(1) LATTICE GAUGE THEORY IN FOUR DIMENSIONS

Abstract

We examine some aspects of four dimensional U(1) lattice gauge theory. Throughout this report we use a pure gauge action without fermions. In the introductory Chapter I we briefly review the general formalism of lattice gauge theory and the current state of knowledge in U(1) lattice gauge theory. We also give a brief account of Monte-Carlo methods and describe some of the numerical techniques to be used in later chapters.

In Chapter II we present results from an analysis of a U(1) model on a simplicial lattice. We comment on the need to consider alternative lattices, briefly describe the simplicial lattice geometry, show that it has the correct naive continuum limit and report on measurements of Wilson loops, string tension and specific heat. We compare our results to those obtained with the more commonly used hypercubic lattice and find good agreement with improved simulation time.

In Chapter III we apply the techniques of the Monte-Carlo Renormalization group to U(1) lattice gauge theory. After a brief introduction to the Real Space Renormalization Group formalism we describe some special numerical techniques which are appropriate to this work. We report on measurements of the model's critical exponents and calculate the renormalized parameters using the Swendsen Method. We discuss the relevance of our results to the

understanding of the U(1) phase diagram in a multi-parameter space.

CONTENTS

	Page
Abstract	2
Acknowledgements	6
Statement of Research Content	7
I. INTRODUCTION	8
1. Quark confinement and lattice gauge theory.	9
2. Review of U(1) lattice gauge theory.	18
3. Monte-Carlo methods.	27
Chapter I Figure Caption	35
Figure	36
II. U(1) GAUGE THEORY ON A SIMPLICIAL LATTICE	37
1. Motivation for alternative lattices	38
2. The simplicial lattice geometry	41
3. Gauge fields and the Action	45
4. Monte-Carlo results	52
5. Summary and conclusions	63
Chapter II Tables	64
Figure Captions	65
Figures	67

	Page
III. THE RENORMALIZATION GROUP AND LATTICE QED	78
1. Introduction	79
2. Background and formalism	80
A. The Real Space Renormalization Group	80
B. Monte-Carlo Renormalization Group methods	88
3. Computational Aspects	97
A. General	97
B. The blocking procedure	99
4. Results and discussion	101
A. The critical exponents	101
B. The renormalized coupling parameters	105
5. Conclusions	109
Chapter III Tables	111
Figure Captions	117
Figures	118
REFERENCES	123

Aknowledgements

I would like to thank Kevin Moriarty for initiating my interest in the subject of lattice gauge theory and guiding my first steps. I would also like to thank Tony Hey and Tony Burkitt for their support and valuable collaboration during the latter part of this work, as well as members of staff and fellow postgraduates in the theory group of Southampton University for their kind hospitality.

I would particularly like to thank Jon Waterhouse and Paul Coddington for helping me unravel the mysteries of the Distributive Array Processor and members of staff at the Royal Holloway and Queen Mary College computer centres, especially Leslie Morgan, Steve Davis and John Steele for their patient assistance.

Thanks are also due to Ian Fox, Thomas Newhaus and Peter Orland for many helpful comments and discussions and, of course, to Elsie Foss for her pen-to-print expertise.

Finally, and most importantly, I would like to thank my parents and Barbara Rowlands for their enormous support over these three years.

Statement of Research Content

Except where credit is explicitly given to another person, all the results presented in this work are derived by the author. Any duplication of results already known but not credited is purely accidental.

CHAPTER I: INTRODUCTION

1. Colour confinement and lattice gauge theory

2. Review of U(1) lattice gauge theory

3. Monte-Carlo methods

1. QUARK CONFINEMENT AND LATTICE GAUGE THEORY

The theoretical and experimental reasons for believing in the existence of quarks and their hitherto unobserved colour degree of freedom are by now well established. In the next few paragraphs we attempt a summary.

(i) Ever since the early days of the simple quark model, it became evident that in order to consolidate the success of that model in describing the hadron spectrum, a new and unobserved degree of freedom (colour) had to be postulated. Thus, it was assumed that each type (flavour) of quark exists in a triplet representation of a colour SU(3) group and that observed hadrons where colour singlets consisting of $q\bar{q}$ (mesons) and qqq (baryons) bound states [1,2].

(ii) The free quark model of ref.[1] has an approximate chiral symmetry under $SU(3)_L \otimes SU(3)_R$ transformations and will therefore reproduce the successful formulation of current algebra and PCAC and the resulting low-energy pion theorems. Furthermore, QCD, the fully interacting theory of quarks and gluons, apart from possessing the well-known symmetries of the strong interaction (parity, charge conjugation, strangeness), is now believed to have all the expected features associated with chiral symmetry breaking [3].

(iii) The predictions of the quark-parton model (and of perturbative QCD) agree very well with experimental studies of deep inelastic lepton-nucleon scattering and electron-positron annihilation processes. This supports the view that quarks behave at high energies (short distances) like free particles and leads to the concept of asymptotic freedom [4].

The discovery that only non-Abelian gauge theories were asymptotically free was probably what led to the acceptance of QCD as a candidate theory of the strong interaction [5]. In order to explain the absence of free quarks in scattering experiments,it was then conjectured that the quarks should be permanently confined within the hadron. However, the confinement mechanism was inaccessible to standard perturbation theory techniques as it involves the long-distance behaviour of QCD where the couplings presumably grow large. Lattice gauge theory, invented by Wegner and Wilson [6,7] provides a much-needed alternative approach which, apart from being independent of perturbation theory, has, as will be seen, certain attractive features of its own [8].

In the lattice approach, space-time is replaced by a discrete, 4-dimensional Euclidean lattice. Gauge fields are defined on the links of the lattice according to the requirements of local gauge invariance. Matter fields may be defined on the sites. As will be seen, confinement is natural in this formalism and the usual continuum QCD will (hopefully) be recovered in the limit of vanishing lattice spacing. Some advantages of the lattice approach are immediately obvious:

– For a lattice of spacing a, a high momentum cut-off $\Lambda \sim 1/a$ is immediately built into the theory at the level of the Lagrangian and before any expansions have begun. Thus, the introduction of the lattice amounts to no more than a regularization scheme which is non-perturbative. We expect the lattice theory to be free of ultraviolet divergences which normally result from the infinite range of momentum integration.

– The gauge fields residing on the links of the lattice may take values from the corresponding Lie group (although discrete groups are also allowed). For the usual SU(n) groups one therefore integrates over a compact manifold and the group integrals are well-defined. The analogous procedure in continuum, locally gauge-invariant field theories introduces a great amount of arbitrariness in the path integral resulting from the extra symmetry. The remedy in that case is to break the local gauge invariance by fixing the gauge (this involves introducing spurious degrees of freedom) and go through a complex procedure involving Ward identities to prove that the resulting physical amplitudes have the desired invariance properties. By contrast, in the lattice approach, not only will the group integration introduce no infinities, but by introducing a spatial cut-off (ie keeping the lattice large but finite) one can formulate the theory in terms of a finite number of well-defined integrals. Thus, lattice gauge theory is well-defined at all times and no gauge-fixing is necessary.

– A gauge theory formulated on a Euclidean lattice resembles a statistical system where physical (thermodynamic) quantities can be extracted from configurational averages. A great deal of knowledge and techniques can be borrowed from the study of similar systems in Condensed Matter Physics. Some of these techniques will be applied later on in this report. In particular, a theory which comprises a finite number of well-defined integrals is accessible to numerical investigation. Indeed much of our knowledge on lattice gauge theories (and of the results included here) is derived from computer simulations.

Against these advantages one must keep in mind that:

– The introduction of the lattice has destroyed the Poincaré invariance which must be regained in the continuum limit.

– There is a great ambiguity in defining a lattice action as many types of action (on many types of lattices) reduce to the same continuum limit when the lattice spacing is naively taken to zero. This, however, in some cases can be used to our advantage, eg for improving the critical behaviour of the lattice theory.

– The problems associated with the inclusion of fermions into the theory are not well understood [9].

– The extrapolation to the zero lattice spacing and infinite lattice limit may be difficult and, in all fairness, is also not well understood.

Despite these shortcomings, lattice results have been so far very promising. There is now numerical evidence for confinement in SU(2) and SU(3) pure gauge theories [10,11] and some preliminary but encouraging results on hadron spectrum calculations [12]. Indeed there is widespread belief that a complete understanding of the strong interaction is now only inhibited by lack of adequate computing power.

In the remainder of this section we review the basic formalism of lattice gauge theory. We concentrate on a pure gauge theory with no fermions. On each link of the lattice characterized by the site n (n = 1,2,...,N, the total number of sites) and direction μ (μ = 1,2,3,4) we place an element of the gauge group SU(N) which we denote $U_\mu(n)$. The inverse element is associated with the opposite direction: $U_\mu^{-1}(n) = U_{-\mu}(n+\hat{\mu})$ where $\hat{\mu}$ is a unit vector in the direction μ. Thus

$$U_\mu(n) = \exp(iB_\mu(n)) \tag{1}$$

where

$$iB_\mu(n) = (i/N)ag_0T^aA_\mu^a \tag{2}$$

and g_0 is the coupling constant, a the lattice spacing, a =

$1,2,\ldots,n^2-1$ and T^a are the group generators in some representation. In this formalism, a local gauge transformation at a site n is a rotation $\chi(n)$. This induces a change in orientation $G(\chi(n))$ in local frames of reference defined at the sites n and $n+\hat{\mu}$

$$U_\mu(n) \rightarrow G(\chi)U_\mu(n)G^{-1}(\chi) \tag{3}$$

Thus, in order to satisfy local gauge invariance (ie be insensitive to arbitrary local changes of orientation) the action must be defined on closed contours of links. Wilson's simplest choice is the basic square formed by four adjacent links (the "plaquette" denoted by $\square$)

$$S = \beta \sum_{\square} \mathrm{tr}U(\square) + \mathrm{h.c.}$$

$$= \beta \sum_{\square} \mathrm{tr}U_\mu(n)U_\nu(n+\hat{\mu})U_{-\mu}(n+\hat{\mu}+\hat{\nu})U_{-\nu}(n+\hat{\nu}) + \mathrm{h.c.} \tag{4}$$

In the present case of a hypercubic lattice, it is easy to show that this action reduces to the correct "naive" continuum limit:

$$S = \frac{1}{4} \int d^4x \, F_{\mu\nu}F_{\mu\nu} \tag{5}$$

where

$$F_{\mu\nu}{}^{a} = \partial_{\mu}A_{\nu}{}^{a} - \partial_{\nu}A_{\mu}{}^{a} - g_{0}f^{abc}A_{\mu}{}^{b}A_{\nu}{}^{c} \qquad (6)$$

and f^{abc} are the group structure constants, provided that

$$\beta = 1/\!\!\int g_{0}{}^{2} \qquad (7)$$

The adjective 'naive' derives from the fact that we have been letting a (the cut-off) tend to zero while keeping the coupling fixed. In Chapter II we illustrate a more interesting similar calculation for a non-hypercubic lattice.

As already mentioned, many other closed-loop operators (possibly associated with different couplings β',β'' etc.) would also preserve local gauge invariance and reduce to the correct naive continuum limit, eq. (5). Thus, the choice of plaquettes in the action is by no means obligatory. (For an alternative formulation, see ref.[13]). Similarly the choice of hypercubic lattice is not the only one, although it is, admittedly, the simplest. Thus, in Chapter II we examine an alternative lattice, the simplicial lattice.

Returning to the action (4), we uncover the physical content of the lattice theory via the partition function

$$Z(\beta) = \int \prod_{n,\mu} [DU_{\mu}(n)] \exp(-\beta S[U]) \qquad (8)$$

where DU is the normalized, invariant group measure and the

product is over all links in the lattice. Expression (8) is well-defined and associates the lattice gauge theory with a corresponding statistical system at temperature T through the identification

$$\beta \propto 1/T \tag{9}$$

This enables the strong coupling limit of the theory to be accessed through high temperature expansions. Some such expansions, to low order, will be used in Chapter II.

Expectation values of gauge invariant operators (Wilson loops) are defined by

$$< W > = Z^{-1} \int \prod_{n,\mu} [DU_\mu(n)]\, W(C) \exp(-\beta S) \tag{10}$$

where C is some closed contour on the lattice and W(C) is a product of oriented link variables along the contour (thus ensuring gauge invariance). $< W >$ is directly related to the potential between two hypothetical static quarks in the lattice as can be seen in a transfer matrix approach

$$V(R) = - \lim_{T\to\infty} (1/T) \ln\langle W(C)\rangle \tag{11}$$

where T is the temporal extent of a static $q\bar{q}$ pair at distance R

apart. $< W >$ can be computed both analytically and numerically and can thus provide information on the interquark forces on the lattice. In particular, an area law behaviour of the type

$$< W(C)> \sim \exp(\chi RT) \qquad (12)$$

where RT is the area enclosed by the loop and χ is the string tension, would signal the onset of a phase with a linearly rising interquark potential. This would be an indication for quark confinement. There is evidence coming from studies of Wilson loops and the string tension that lattice gauge theory confines electrons [10,11] as well as quarks. It is therefore essential to show that there is a phase transition in lattice QED separating the two phases of linearly rising and inverse square law potential, but that no such transition exists in QCD where confinement must be shown to persist throughout the coupling range and into the asymptotic freedom regime ($g\sim 0$). Numerical investigations on pure gauge systems have indicated that in the case of an Abelian lattice theory the string tension would indeed vanish at weak couplings (finer lattices) in the thermodynamic limit but for non-Abelian theories there is a narrow range in the couplings where the string tension changes from a behaviour predicted by strong coupling expansions to one predicted by the renormalization group. This is taken as positive evidence for the onset of asymptotic freedom but a definite conclusion on the absence of a deconfining phase transition is still premature.

2. REVIEW OF U(1) LATTICE GAUGE THEORY

In this section we review the current state of knowledge for U(1) lattice gauge theory. Owing to the large volume of existing literature, we have adopted a selective approach and concentrated on those topics that are relevant to results and discussions presented elsewhere in this report.

There are several motivations for the study of U(1) lattice gauge theory. Firstly, it is the lattice version (albeit without fermions) of the prototype gauge theory, Quantum Electrodynamics (QED). A great deal is known today about QED because of its relative simplicity and its accessibility to perturbative methods. In this connexion, a study of its lattice version, provides a test of the correctness of the lattice approach. Secondly, lattice QED is an ideal ground for the study of the deconfining phase transition which takes place at a relatively small value of β (coarser lattice). By contrast, in non-Abelian gauge theory, that transition, if it exists at all, must occur at a much larger value of β , thus requiring correspondingly larger lattices for investigation. Finally, U(1) is the group of phase factors, so in numerical studies one deals with numbers, rather than matrices, resulting in substantial savings in simulation time. These savings can be made even greater given that for a substantial range of couplings, including the phase transition, U(1) lattice gauge theory is well approximated by a discrete subgroup Z(N). This is exploited in the calculations of Chapter III.

As mentioned in Section 1, the Wilson loops in the strong coupling limit of U(1) (or indeed of any lattice gauge theory) display an area law behaviour which is also confirmed by strong coupling expansions. Conversely, in the weak coupling regime the Wilson loops change to a behaviour compatible with a Coulomb-type interaction. The single transition point seen around $\beta \simeq 1.0$ separates the confining phase from a QED-like phase containing massless photons. It was subsequently proved rigorously [14] that U(1) does have a phase transition. Absence of such rigorous proof would render lattice gauge theory somewhat suspect. However the nature of this phase transition and its driving mechanism, as well as the precise location of the critical point, remain to be determined. Furthermore, the extent of the influence (if any) of the critical properties of U(1) lattice gauge theory on electrodynamics is unclear. The purpose of this report is to contribute to an increased understanding on these matters.

Specializing to the case of U(1) symmetry with the parametrization $U_\mu(n) = \exp(i\theta_\mu(n))$ the Wilson action (4) reduces to

$$S = \beta \sum_{\square} \cos\theta_{\square} \tag{13}$$

where $\square$ stands for plaquette and $\cos\theta_{\square}$ is the cosine of the sum of oriented angles round the plaquette. The identificatrion

$$\beta = 1/e_0^2 \tag{14}$$

where e_0 is the bare charge, results in the correct naive continuum limit ($a \to 0$)

$$S = \tfrac{1}{4} \int F_{\mu\nu} F_{\mu\nu} \, d^4x \qquad (15)$$

where $F_{\mu\nu}$ is the usual electromagnetic field tensor. In this formulation the electromagnetic potentials are of manifestly angular nature:

$$iae_0 A_\mu(n) = i\theta_\mu(n) \qquad (16)$$

As already mentioned, the naive continuum limit (15) is an encouraging first step but in itself is no indication that the action (13) is a possible lattice version of electrodynamics. In order to prove this, one would have to study the phase diagram of U(1) lattice theory very thoroughly, develop a renormalization group for it and show that the spin-wave phase of eq.(13) has the same long-distance properties as eq.(15). This procedure is very difficult and has not been done in a convincing manner although approximate discussions have appeared which tend to support this conjecture [15].

Early Monte-Carlo investigations with the action (13) provided evidence that the theory underwent a second order phase transition (corresponding to an infinite correlation length) at approximately $\beta \simeq 1$. That evidence came from several sources. Firstly, a hysteresis analysis by Creutz et al [16] indicated a transition with no associated latent heat. A finite size scaling

analysis of the specific heat by Lautrup and Nauenberg [17] also indicated a second order phase transition with an associated correlation length critical exponent $\nu \simeq 1/3$. These results were later supported by more detailed Monte-Carlo analyses of the Wilson action by Moriarty [18] and the same conclusion was also reached by Bhanot [19] and by Caldi [20] through a finite size scaling analysis of the Wilson loops and the string tension. Bhanot also showed that the theory has a line of critical points in the spin wave phase at each of which, a scale invariant continuum theory could be defined. All these studies were based on straightforward Monte-Carlo simulations with the Wilson action and indicated a second order phase transition with an infinite correlation length. In Chapter II we present similar results in connexion with the simplicial lattice. However, later studies with an extended action revealed a rich phase structure and suggested that a complete understanding of the U(1) phase diagram requires the use of more powerful analytic and numerical techniques.

A somewhat separate line of research was initiated by Banks, Myerson and Kogut [15] who, starting with the Villain action [21] showed that the U(1) phase transition is driven by topological excitations and is therefore of the Kosterlitz-Thouless type [22] which is known to occur in the two dimensional X-Y model. Specifically to the U(1) model they showed that the strong coupling region is populated by unbound monopole current loops. This results in a screening of the magnetic fields and the confinement of the electric flux into flux tubes. Thus the strong coupling limit of U(1) resembles the magnetic analog of a superconductor

whereas in the weak coupling phase it was shown that the monopole current loops are suppressed and electric flux breaks out into the familiar Coulombic pattern. A Monte-Carlo analysis by De Grand and Toussaint [23] showed that the monopole density undergoes a sharp change at the transition point. Hopefully, in the case of non-Abelian gauge theory the 'superconductor picture' persists throughout the coupling range.

A great deal of work has been done towards establishing parallels between periodic QED and the X-Y model and towards an increased understanding of the role of the monopoles as the driving mechanism for the phase transition. It was shown by Cardy [24] that the coupling constant α of U(1) is renormalized by the monopoles and that it is analogous to the critical exponent η of the X-Y model. It was then found by Luck [25] by means of a low temperature expansion that the renormalized squared charge took a universal value at the deconfining point equal to $4\pi\alpha_c=1.9\pm0.1$ Numerical studies on the monopoles include the work of Barber [26] who found a strong correlation between the fluctuations in the average plaquette action and the monopole number density and Barber et.al.[27] who showed that four dimensional U(1) lattice theory without monopoles undergoes no phase transition.

Recently, in a high statistics calculation, Jersak, Newhaus and Zerwas [28] showed that very near the transition point the average plaquette undergoes a small hysteresis over a narrow range of couplings. This, together with the fact that there appeared to be two stable states on either side of the phase transition, was taken as evidence that previous analyses had overlooked the

possibility of the transition being first order. However it is difficult to separate the genuine thermodynamic limit results from finite size effects. These studies pointed to the need for investigating an 'extended' Wilson action with more than one coupling. Bhanot was the first to examine a two-coupling action [29]

$$S = \tfrac{1}{2}\beta \sum_{\square} (U + U^{+}) + \tfrac{1}{2}\gamma \sum_{\square} (U^{2} + U^{+2}) \qquad (17)$$

where the γ-term is known as the 'adjoint' coupling. He found the phase diagram reproduced in Fig.1. From simple symmetry considerations it can be shown that the phase diagram is symmetric under $\beta \to -\beta$ and under reflection through the origin at $\beta=0$. It can also be easily seen by inspection of eq.(17) that in the $\gamma \to \infty$ limit the theory coincides with Z(2).

The lines DZ, EF, and BC in Fig.1 are second order phase transitions whereas AC and DC are first order. The discontinuity in the average plaquette decreases along the line CD. The diagram shows that there is no way to pass from the confining phase at small β and γ to the spin-wave phase at large β and $|\gamma|$ without crossing a phase transition. Qualitatively similar results were obtained through a mean-field approach by Dagotto [30].

Evertz et.al.[31] did a thorough examination of the action eq.(17). They measured the discontinuity in average plaquette in the interval $0.2 < \gamma < 0.5$ and extrapolated according to a power law. They find that the discontinuity vanishes at the point X ,

shown in Fig.1 which they locate at $\beta = 1.09 \pm 0.04$ and $\gamma = -0.11 \pm 0.05$. The negative value of γ means that the transition at the Wilson axis is still first order, albeit very weakly. Evertz et.al. claim that point X is tricritical and estimate the associated tricritical exponents [32].

In the light of the results presented in ref.[31] it becomes clear that whether the phase transition on the Wilson axis is first or second order, it is dominated by the nearby tricritical point. Straightforward Monte-Carlo investigations are generally unreliable when dealing with tricritical behaviour as evidenced by similar studies in spin systems [33]. This is because the scaling laws in the vicinity of a tricritical point (or, more generally, of a multi-critical point) have to take into account the presence of many critical lines emerging from that point. This leads to cross-over phenomena which are difficult to interpret. Depending upon the way the tricritical point is approached, one defines two new sets of critical exponents:

(i) Tricritical exponents, usually denoted by subscript t, govern the approach to the tricritical point along any path not asymptotically parallel to the phase boundary.

(ii) Subsidiary exponents denoted by u, are associated with an approach along the triple line.

For instance, at the tricritical temperature T_{TCP} the correlation length behaves as

$$\xi \sim | T - T_{TCP} |^{-\nu_t} \qquad (18)$$

with $\nu_t \neq \nu$ in general. A discontinuity along the triple line (say in magnetization) is given by

$$\Delta M \sim | T - T_{TCP} |^{\beta} \tag{19}$$

These exponents satisfy a hyperscaling relation

$$\beta_u = \phi(\nu_t d - 1) \tag{20}$$

where ϕ is known as the cross-over exponent. By a scaling analysis on the latent heat, Evertz et.al. found

$$\beta_u = 1.7 \pm 0.2 \qquad \phi = 1.5 \pm 0.3 \tag{21}$$

This gives a value for ν_t approximately equal to 0.53 which is closer to the classical value of $\frac{1}{2}$ rather than $^1/_3$.

In conclusion, we can summarize the problems which must be addressed to in a full investigation of U(1) lattice gauge theory as follows:

- The precise location of the tricritical point. Is it a tricritical or a multi-critical point?
- The computation of the associated tricritical and subsidiary exponents.
- The determination of the phase diagram in a larger, multi-coupling constant space.
- The determination of the renormalization group flows and of the changes of critical exponents along them.

In Chapter II we examine the U(1) gauge theory with the simple Wilson action on a simplicial lattice. In Chapter III we employ the more powerful methods of Monte-Carlo Renormalization Group using an extended action with five coupling constants.

3. MONTE-CARLO METHODS

Since a good part of this report is devoted to Monte-Carlo analysis, we include here a brief collection of facts and background to Monte-Carlo methods [34].

The Monte-Carlo (MC) method as applied to problems in statistical physics provides a way of performing multi-dimensional functional integrals by 'importance sampling' over the entire configuration space. Consider a system described by an action S, containing a set of dynamical degrees of freedom U:

$$S[U] = \sum_{a} K_a S_a \qquad (22)$$

where the S_a are various combinations of the U's and factors like the inverse temperature times the Boltzmann constant have been included in the definition of the couplings K_a . The simplest example is the nearest neighbour (a = 1) Ising model (U = ± 1)

$$S_1 = S_{\text{nearest neighbour}} = \sum_{<ij>} U_i U_j \qquad (23)$$

The equilibrium probability can be written as

$$P[U] = Z^{-1} \exp(-\beta S[U]) \qquad (24)$$

where $\mathbf{Z}$ is the (unknown at this stage) partition function. Correlation functions can now be defined as weighted configurational sums, eg

$$< S_\alpha > = \sum_{[U]} S_\alpha[U]\, P[U] \qquad (25)$$

However, direct summation is impractical here because of the exceedingly large number of configurations, even for simple systems. For example a 3-d Ising system on a 10 x 10 x 10 lattice has 2^{1000} configurations. Monte-Carlo is effectively an efficient way of sampling eq.(24). The weighted distributions in eq.(25) then become unweighted averages over properly selected configurations.

The process of selecting configurations begins by placing each of the dynamical variables U in contact with a heat bath at the appropriate temperature. After each dynamical variable has come into contact with the reservoir a sufficient number of times, the system will come to equilibrium with the desired probability distribution. So the problem is to generate a stochastic sequence of configurations whose probability distribution converges to eq.(24):

$$P(U,t) \rightarrow P(U) \text{ as } t \rightarrow \infty \qquad (26)$$

Now the time development of the probability of finding any particular configuration U at time t is described by a master equation

$$P(U,t+\delta t) = P(U,t) + \sum_{U'} \left[W(U',U)P(U',t) - W(U,U')P(U,t) \right] \qquad (27)$$

where P(U,t) is the probability of finding configuration U at time t and W(U',U) is the transition rate from U' to U during time interval δt. In order to ensure that (26) is asymptotically satisfied we impose the (sufficient but not necessary) condition of detailed balance:

$$W(U',U)P(U') = W(U,U')P(U) \qquad (28)$$

This leads to a very simple algorithm, as, using (24) we find

$$\frac{W(U,U')}{W(U',U)} = \exp\{-(S[U']-S[U])\} \qquad (29)$$

where the normalization constant Z cancels. A particularly attractive feature of this formulation is that local changes in the configuration affect only those local degrees of freedom involved and it is not necessary to calculate the entire action at every stage. This feature allows for efficient algorithms to be designed

even for complicated models with many interactions. This is an important advantage of the MC method as opposed to, say, real space renormalization group methods.

There are several ways to implement the detailed balance condition (29). Two of the most transparent are the Metropolis algorithm [35] and the heat bath algorithm [36]:

(i) In the Metropolis algorithm we select a particular variable U_i from the configuration U and then we generate a candidate new value $\hat{U}_i$ with an arbitrary probability distribution. We then compute the change in action δS effected by the replacement of U_i by $\hat{U}_i$:

$$\delta S = S[\hat{U}_i] - S[U_i] \qquad \text{all other variables fixed} \qquad (30)$$

If $\delta S \leq 0$ the change is accepted. Otherwise a pseudo-random number r is generated in the interval between 0 and 1 with uniform probability and:

$$\begin{aligned} &\text{if } r \leq e^{-\delta S} \quad \text{the change is accepted} \\ &\text{if } r > e^{-\delta S} \quad \text{the change is rejected} \end{aligned} \qquad (31)$$

It is easy to check that this procedure satisfies the detailed balance condition (29). We then move systematically through the lattice until all the variables U_i have been accessed. In this algorithm the aim is to move as quickly as possible to configurations with lower action. Its efficiency is therefore limited by

the fact that in a weak coupling regime low-action configurations are favoured and most of the changes may lead to a substantial increase in the action thus resulting in many rejections. This problem is briefly addressed in Chapter II. Also in Chapter II we examine a 'modified' Metropolis algorithm, where one updates a given variable several times before moving on to the next variable. This of course increases the probability of acceptance. The advantage of performing several updates per step rather than doing more steps lies in the reduced amount of overheads involved with referencing the dynamical variables which are usually stored in large multi-dimensional arrays. The Metropolis algorithm is used in Chapter III.

(ii) In the heat bath method the new value U_i' is selected among all possible values for that variable with a probability distribution proportional to $\exp[-S(U_i')]$, all other variables being kept fixed. Thus the value of the old variable U_i plays no part in the determination of the new variable and detailed balance is satisfied in an obvious way. The problem is to evaluate the new variable computationally on the basis of a given probability distribution. Here we illustrate the method for the particular case of a U(1) gauge theory, as applied in Chapter II. The method is based on the von Neumann acceptance-rejection criterion [37]. Denote by $U' = e^{i\theta'}$ the new U(1) element to be associated with a given link, all other links being kept fixed. We consider the probability distribution

$$dP(U') = dU' \exp(\beta S[U'])$$

$$= d\theta' \exp\left(\beta \mathrm{Re}\left[e^{-i\theta'} X e^{i\bar{\theta}} \right]\right) \qquad (32)$$

where $Xe^{i\bar{\theta}}$ expresses the sum of products of the three fixed links of a plaquette, $\bar{\theta}_{\square}$, over all (six) plaquettes sharing that link:

$$X e^{i\bar{\theta}} = \sum_{i=1}^{6} e^{i\bar{\theta}_{\square}} \qquad (33)$$

Hence we want to generate a random number with the distribution

$$dP(\tilde{\theta}) = \exp(\beta X \cos\tilde{\theta})\, d\tilde{\theta} \qquad (34)$$

where $\tilde{\theta}=\theta-\theta'$. It is preferable to normalize the distribution so as to be less or equal to 1, so we consider instead

$$dP(\tilde{\theta}) = \exp(\beta X(\cos\tilde{\theta}-1))d\tilde{\theta} \qquad (35)$$

Thus, we first generate a random number r in the interval (0,1) and assign

$$\tilde{\theta} = 2\pi r \qquad (36)$$

Then we generate a second random number r′ and if $\exp[\beta X(\cos 2\pi r -1)] < r'$, r is rejected and the whole procedure is repeated until the above criterion is satisfied. This procedure yields the desired distribution and was found to be very effective.

There are two major limitations in the MC approach. The first concerns the long relaxation times near criticality and results in successive measurements being correlated. Naturally one must ensure that total simulation times are much longer than the longest relaxation time. This, in most cases, is possible within the framework of modern computers. Moreover the correlation effects can be controlled and measured [38,39]. In Chapters II and III we shall present some results from such an analysis.

The second limitation of MC methods is more severe and concerns finite size effects [40]. Naturally in a computer simulation one uses a finite lattice. However as the critical region is approached, the correlation length grows and eventually exceeds the size of the lattice. In that case, calculated thermodynamic functions are no longer characteristic of the bulk of the system, the computed expectation values deviate from those of the infinite system and critical singularities are rounded off. (In fact it can be rigorously proved, but it is also intuitively obvious, that in a finite lattice there can be no phase transition since with a finite number of finite integrals the partition function is everywhere analytic.) Hence, finite size effects will be important unless one works in a region of the couplings where

$$a \ll \xi \ll L \tag{37}$$

where a is the lattice spacing, and L is the linear dimension of the lattice. The inequality $a \ll \xi$ can be relaxed by suitably modifying the lattice action [41]. The condition $\xi \ll L$ is also

difficult to deal with. One way to bypass it is to use finite size scaling analysis [42]. The main assumption here is that near the critical point the correlation length does not diverge but becomes of the order of the lattice size. As regards the specific heat for example, one simulates at the critical temperature and calculates the dependence of the peak on the linear size of the system

$$C(T_c) \sim L^{\beta/\nu} \tag{38}$$

where ν is a critical exponent. This however still suffers from statistical errors as it is difficult to pinpoint the peaks accurately enough to extract ν. A much more powerful approach for obtaining meaningful information from small lattices involves the Monte-Carlo Renormalization Group which is the subject of Chapter III.

FIGURE CAPTION

Fig. 1: Approximate representation of the U(1) lattice gauge theory phase diagram in the fundamental-adjoint plane (after ref.[29]). The broken lines represent first order phase transitions and the solid lines correspond to continuous phase transitions. The point X near the fundanental (Wilson) axis, is claimed to be tricritical [31].

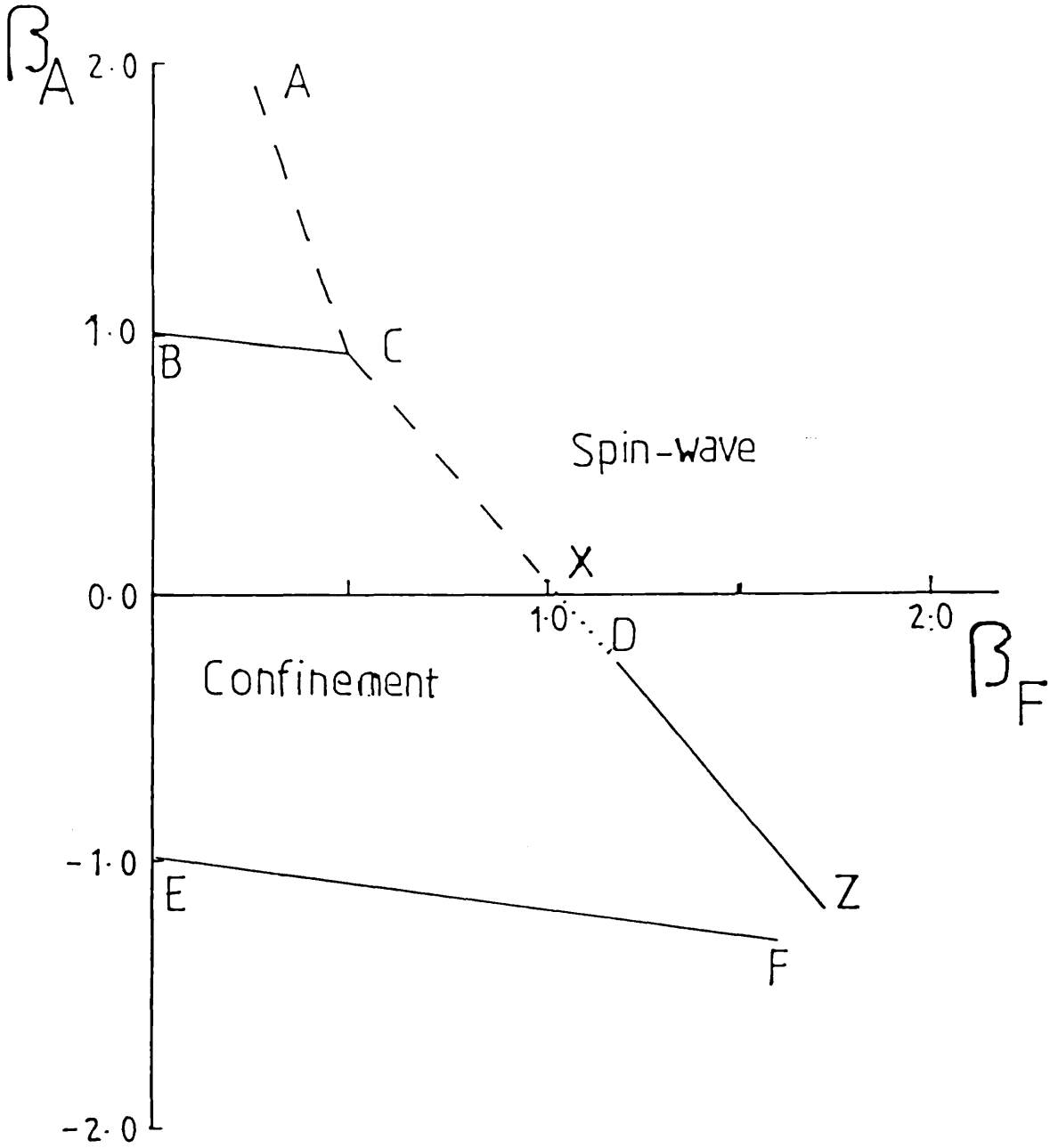
β_A
2·0
1·0
0·0
-1·0
-2·0
A
B
C
X
D
Z
E
F
Spin-wave
Confinement
1·0
2·0
β_F

Fig. 1

CHAPTER II: U(1) GAUGE THEORY ON A SIMPLICIAL LATTICE

1. Motivation for Alternative Lattices

2. The Simplicial Lattice Geometry

3. Gauge Fields and the Action

4. Monte-Carlo Results

5. Summary and Conclusions

1. MOTIVATION FOR ALTERNATIVE LATTICES

Lattice calculations both numerical and analytic have traditionally been performed on a regular hypercubic lattice. Undoubtedly the hypercubic lattice provides the simplest and most transparent regularization of gauge theories in four dimensions.

However, there have been some attempts towards alternative constructions. Thus, Christ, Friedberg and Lee [43] consider a lattice with randomly distributed points whereas Celmaster [44] uses a body centred tesseract lattice. In the following sections we report on results obtained with the simplicial lattice [45, 46].

The common feature of the above construction is its greater geometric complexity, especially in four dimensions. However, alternative lattices are interesting as they should provide an independent check on both analytic and numerical calculations. In particular (as physics must not depend on the choice of regulator) universality can be tested by comparing the results on a hypercubic lattice with those obtained on a simplicial lattice.

Apart from universality considerations, the simplicial lattice is worth studying in its own right. It has a much larger point-symmetry group than the hypercubic lattice and consequently, as Celmaster pointed out, a better rotational invariance. The singularities associated with the restoration of rotational invariance (in particular the roughening transition [47]) are therefore expected to be weaker and the onset of continuum physics to take place at larger values of beta, ie coarser lattices. Thus,

we expect strong coupling expansions to be more regular, giving better accuracy with less terms and should hopefully be more easily continued from the strong coupling to the asymptotic freedom regime. We also note that the simplicial lattice has two different kinds of two-planes which may be used independently when computing the string tension. As will be shown in the next section, one of these sets of plane contains triangular Wilson loops whereas in the other the Wilson loops are rectangles. Thus, by comparing the string tensions, we have a way of checking rotational invariance.

The more densely packed nature of the simplicial lattice confers several advantages over the hypercubic lattice. There are now more plaquettes per orientation and each link interacts with more neighbours. We therefore expect mean field theory to provide better results at lower dimensionalities. For the same reason, we expect numerical benefits. As fluctuations become less important, Monte-Carlo simulations should thermalize more rapidly, the specific heat should be smoother and more regular and we should be able to extract reliable continuum limit results with good statistics from smaller lattices and with fewer data points.

In this chapter we study some aspects of the U(1) gauge theory formulated on the simplicial lattice. In Section 2 we describe the simplicial lattice geometry. We only emphasize those aspects which are useful for numerical work. In Section 3 we define the simplicial lattice action and show that it has the

correct continuum limit. Section 4 contains results from a Monte-Carlo analysis. Finally in Section 5 we summarize our conclusions.

2. THE SIMPLICIAL LATTICE GEOMETRY

In this section, we shall be denoting the simplicial lattice basis vectors in d dimensions by $\{ \vec{\varepsilon}_i \}$ and the basis vectors of the corresponding hypercubic lattice by $\{ \vec{e}_i \}$

The d-dimensional simplicial lattice is obtained from a (d+1)-dimensional hypercubic lattice by projecting its basis vectors $\{\vec{e}_1, \vec{e}_2, \ldots, \vec{e}_{d+1}\}$ onto the hyperplane orthogonal to the vector $\{\vec{e}_1+\vec{e}_2+ \ldots +\vec{e}_{d+1}\}$. This hyperplane is now a physical d-dimensional space in which we can define a redundant basis.

$$\vec{\varepsilon}_i = \vec{e}_i + (\vec{e}_1 + \ldots +\vec{e}_{d+1})/(d+1) \qquad (1)$$

for the simplicial lattice, obeying the constraint

$$\vec{\varepsilon}_1 + \vec{\varepsilon}_2 + \ldots + \vec{\varepsilon}_{d+1} = 0 \qquad (2)$$

Thus, the $\{\vec{\varepsilon}_i\}$ are effectively a basis for a d-dimensional space. It is easy to show from the definition (1) that

$$\vec{\varepsilon}_i^{\,2} = d/(d+1) \quad \text{and} \quad \vec{\varepsilon}_i.\vec{\varepsilon}_j = -1/(d+1) \qquad (3)$$

Two particular cases are well-known. In dimension d=2 we have a traingular lattice. In d=3 the simplicial lattice reduces to an fcc lattice. In the following we shall denote by a the spacing of the hypercubic lattice and by b the spacing of the resulting simplicial lattice. These are related by

$$b = \sqrt{2}\, a \tag{4}$$

Sites in the simplicial lattice are identified with integers $\{n_i, i=1,2,\ldots,d+1\}$ with $\Sigma\, n_i = 0$. Thus, the sites are located by position vectors $\vec{r}$ where

$$\vec{r} = a \sum_{i=1}^{d+1} n_i \vec{e}_i = a \sum_{i=1}^{d+1} n_i \vec{\epsilon}_i \quad \text{with} \quad n_{d+1} = -n_1 - \ldots - n_d \tag{5}$$

Periodic boundary conditons can be most easily implemented by constraining the n_i's in the range

$$0 \leq n_i < L$$

where L is the linear dimension of the lattice. This yields the total number of sites in the lattice to be

$$N = L^d \tag{6}$$

Nearest neighbours are separated by $a\vec{\epsilon}_{ij} = a(\vec{\epsilon}_i - \vec{\epsilon}_j)$ (with $i \neq j$

and i,j = 1,2, ..., d+1). Thus the simplicial lattice spacing, as stated in eq.(4) is $b = \sqrt{2}a$. There are Nd(d+1) nearest neighbours in the lattice separated by $\sqrt{2}a$. Thus the simplicial lattice has $\frac{1}{2}Nd(d+1)$ links.

Triangles: In the two-planes ($\vec{\epsilon}_{ij}$, $\vec{\epsilon}_{jk}$) with i, j, k=1, ...,d+1 and all different, the section of the lattice gives a triangular lattice. There are $Nd(d^2-1)/6$ such directions characterized by (i,j,k) with $1 \leq i<j<k \leq d+1$. Hence there are $Nd(d^2-1)/3$ triangles on the lattice and a link in the direction (ij) bonds 2(d-1) triangles labelled in pairs by k (k=1,...,d+1; $k \neq i, k \neq j$), (Fig. 1a)

Squares In the two-planes ($\vec{\epsilon}_{ij}$, $\vec{\epsilon}_{kl}$) with i,j,k,l = 1,...,d+1 and all different, we have a square lattice. There are $Nd(d^2-1)(d-2)/8$ such directions characterized by (i,j,k,l) with ($1 \leq i<j \leq d+1$) and ($1 \leq k<l \leq d+1$). Hence the simplicial lattice has $Nd(d^2-1)(d-2)/8$ squares and a link in the direction (ij) bonds (d-1)(d-2) squares labelled in pairs (k,l) with k,l=1,...,d+1 (Fig. 1b)

Volume per lattice site A given lattice site, specified by a set of (integer) coordinates (n_i, i=1,...,d+1) is located at

$$a \sum_{i=1}^{d+1} n_i \vec{\epsilon}_i = a \left[\sum_{i=1}^{d} n_i \vec{\epsilon}_i + (n_1+\ldots+n_d)(\vec{\epsilon}_1+\ldots+\vec{\epsilon}_d) \right]$$

(using (2) and (5))

$$= a \sum_{i=1}^{d} (n_1 + \quad + n_d) \vec{\epsilon}_i$$

$$= a \sum_{i=1}^{d} n_i' \vec{\varepsilon}_i$$

Thus, the n_i's define the n_i''s uniquely. We note that $\Sigma\, n_i' = (d+1)(n_1+\ldots+n_d)$ is a multiple of (d+1). So we have a regular lattice with basis $(a\vec{\varepsilon}_1,\ldots,a\vec{\varepsilon}_{d+1})$ with only a 1/(d+1) fraction of the sites occupied. The volume per lattice site is therefore $[(d+1)\det(a\vec{\varepsilon}_i.a\vec{\varepsilon}_j)]^{1/2}$. From (3), we find finally

$$\text{Volume/Site} = a^d \sqrt{(d+1)} \qquad (7)$$

The geometrical properties of the simplicial lattice (as well as the corresponding properties of the hypercubic lattice, for comparison) are summarized in Table 1.

3. GAUGE FIELDS AND THE ACTION

The simplicial lattice pure gauge action is written in the standard way as a sum of products of gauge group elements round elementary closed paths (triangular and square plaquettes)

$$S = \frac{\beta}{2N} \sum_{\Delta} \mathrm{tr}(UUU) + \frac{\gamma}{2N} \sum_{\square} \mathrm{tr}(UUUU) \qquad (8)$$

where the sums are over oriented plaquettes and N is the dimension of the fundamental representation of the gauge group. The U's are associated with every site (S) and for each of the d(d+1)/2 directions (ij). We associate the inverse element U^+ with the opposite direction (ji). Thus

$$U \to U(s,(ij)) = U^+ (s+m_i-m_j,(ij))$$

This action has the desired properties of locality and gauge invariance as discussed in Chapter I. It seems, however, that there are too many degrees of freedom as in the continuum limit A_μ has only d, rather than d(d+1)/2 components. Therefore, it is not obvious that the action (8) reduces to the correct naive continuum limit. In this section we show that the remaining d(d-1)/2 degrees of freedom decouple from the theory and do not propagate as $a \to 0$. To this end, we parametrize

$$U(s,(ij)) = \exp\{ia\epsilon_{ij}{}^{\mu}\mathcal{A}_{\mu}(X)+ia^2\epsilon_i{}^{\mu}\epsilon_j{}^{\nu}\mathcal{T}_{\mu\nu}(X)\} \qquad (9)$$

where X is the centre of the link $(s,(ij))$. $\mathcal{A}_{\mu}$ and $\mathcal{T}_{\mu\nu}$ belong to the Lie Algebra of the gauge group and $\mathcal{T}_{\mu\nu}$ is antisymmetric, so it has the correct number of components, ie $d(d-1)/2$.

We first calculate the triangular part of the action. We evaluate the link variables at the centre X of the triangle (ijk) (Fig.2). Using all contributions at X and keeping terms up to $O(a^2)$ we get

$$U(s,(ij)) = \exp\{ia\epsilon_{ij}{}^{\mu}\mathcal{A}_{\mu}(X)+ia^2\epsilon_i{}^{\mu}\epsilon_j{}^{\nu}\mathcal{T}_{\mu\nu}(X)$$

$$\pm(ia^2/6)\epsilon_{ij}{}^{\mu}(\epsilon_{ki}{}^{\nu}+\epsilon_{kj}{}^{\nu})\,\partial_{\nu}\mathcal{A}_{\mu} + \ldots \qquad (10)$$

Then, by the Baker-Campbell-Haussdorff relations we can evaluate after some algebra, the triangular part of the action

$$UUU = \exp\{\, ia\mathcal{A}_{\mu}\ (\epsilon_{ij}{}^{\mu} + \epsilon_{jk}{}^{\mu} + \epsilon_{ki}{}^{\mu}\ )$$

$$\pm(ia^2/12)(\partial_{\mu}\mathcal{A}_{\nu}-\partial_{\nu}\mathcal{A}_{\mu})[\epsilon_{ij}{}^{\nu}(\epsilon_{ki}{}^{\mu}+\epsilon_{kj}{}^{\mu}) + \text{cyclic}(i,j,k)]$$

$$-(a^2/2)\,[\mathcal{A}_{\mu}\,,\mathcal{A}_{\nu}](\epsilon_{ij}{}^{\mu}\epsilon_{jk}{}^{\nu}+\epsilon_{ij}{}^{\mu}\epsilon_{ki}{}^{\nu}+\epsilon_{jk}{}^{\mu}\epsilon_{ki}{}^{\nu})$$

$$+ia^2\mathcal{T}_{\mu\nu}(\epsilon_i{}^{\mu}\epsilon_j{}^{\nu} + \epsilon_j{}^{\mu}\epsilon_k{}^{\nu} + \epsilon_k{}^{\mu}\epsilon_i{}^{\nu})$$

$$+ O(a^3)\ \} \qquad (11)$$

The term linear in A_μ vanishes because of antisymmetry. Define

$$\sigma_{ijk}{}^{\mu\nu} \equiv \varepsilon_{ij}{}^{\mu}\varepsilon_{jk}{}^{\nu} = \varepsilon_{jk}{}^{\mu}\varepsilon_{ki}{}^{\nu} = \varepsilon_{ki}{}^{\mu}\varepsilon_{ij}{}^{\nu} \qquad (12)$$

it can easily be seen that $\varepsilon_i{}^{\mu}\varepsilon_j{}^{\nu}+\varepsilon_j{}^{\mu}\varepsilon_k{}^{\nu}+\varepsilon_k{}^{\mu}\varepsilon_i{}^{\nu} = \sigma_{ijk}{}^{\mu\nu}$.

We finally find

$$UUU = \exp\{ \pm ia^2\sigma_{ijk}{}^{\mu\nu} (\tfrac{1}{2} F_{\mu\nu} + T_{\mu\nu}) \} \qquad (13)$$

where

$$F_{\mu\nu} = \partial_\mu A_\nu - \partial_\nu A_\mu + i[A_\mu, A_\nu] \qquad (14)$$

The square part of the action can be evaluated in a similar manner. Calculating at the centre X of the square we have

$$U(s,(ij)) = \exp(ia\varepsilon_{ij}{}^{\mu}A_\mu(X) + ia^2\varepsilon_i{}^{\mu}\varepsilon_j{}^{\nu} T_{\mu\nu}(X)$$

$$+ \tfrac{1}{2}ia^2\varepsilon_{ij}{}^{\mu}\varepsilon_{lk}{}^{\nu} \partial_\nu A_\mu + \dots) \qquad (15)$$

Thus,

$$U_{ij}U_{kl}U_{jl}U_{lk} = \exp\{ ia A_\mu(\varepsilon_{ij}{}^{\mu}+\varepsilon_{kl}{}^{\mu}+\varepsilon_{ji}{}^{\mu}+\varepsilon_{lk}{}^{\mu})$$

$$+ \tfrac{1}{2}a^2 i(\partial_\mu A_\nu - \partial_\nu A_\mu)(\varepsilon_{ij}{}^{\nu}\varepsilon_{lk}{}^{\mu} - \varepsilon_{ij}{}^{\mu}\varepsilon_{lk}{}^{\nu} + \varepsilon_{kl}{}^{\nu}\varepsilon_{ij}{}^{\mu} - \varepsilon_{kl}{}^{\mu}\varepsilon_{ij}{}^{\nu})$$

$$-\tfrac{1}{2}a^2 [A_\mu, A_\nu](\varepsilon_{ij}{}^{\mu}\varepsilon_{kl}{}^{\nu} + \varepsilon_{ij}{}^{\mu}\varepsilon_{ji}{}^{\nu} + \varepsilon_{ij}{}^{\mu}\varepsilon_{lk}{}^{\nu} + \varepsilon_{kl}{}^{\mu}\varepsilon_{lk}{}^{\nu}$$

$$+\varepsilon_{ij}{}^{\mu}\varepsilon_{lk}{}^{\nu})$$

$$+ia^2\mathcal{T}_{\mu\nu}(\varepsilon_i{}^{\mu}\varepsilon_j{}^{\nu}+\varepsilon_k{}^{\mu}\varepsilon_l{}^{\nu}+\varepsilon_j{}^{\mu}\varepsilon_i{}^{\nu}+\varepsilon_l{}^{\mu}\varepsilon_k{}^{\nu})$$

$$+ O(a^3)\} \qquad (16)$$

where the term in $\mathcal{T}_{\mu\nu}$ and, as before, the linear term in $\mathcal{A}_{\mu}$ vanish. Introducing the antisymmetric tensor

$$\sigma_{ijkl}{}^{\mu\nu} \equiv \varepsilon_{ij}{}^{\mu}\varepsilon_{kl}{}^{\nu} \qquad (17)$$

we find

$$UUUU = \exp\{\, ia^2\sigma_{ijkl}{}^{\mu\nu}\,\tilde{\mathcal{F}}_{\mu\nu}\,\} \qquad (18)$$

The action is therefore given by

$$S = (\beta/2\mathcal{N}) \sum_{\Delta} \mathrm{tr}\{\exp[\pm ia^2\sigma_{ijk}{}^{\mu\nu}(\tfrac{1}{2}\mathcal{F}_{\mu\nu} \pm \mathcal{T}_{\mu\nu})]\}$$

$$+ (\gamma/2\mathcal{N}) \sum_{\square} \mathrm{tr}\{\exp[ia^2\sigma_{ijkl}{}^{\mu\nu}\,\tilde{\mathcal{F}}_{\mu\nu}]\}$$

Expanding the exponential gives first a constant, irrelevant term, then at order a^2 a term which reverses sign by reversing the orientation and so it does not contribute. The next term is of order a^4:

$$\mathrm{tr}[-(\beta/4N)a^4 \sum_{\Delta} \sigma_{ijk}^{\mu\nu}\sigma_{ijk}^{\rho\sigma} (\tfrac{1}{2}F_{\mu\nu} \pm T_{\mu\nu})(\tfrac{1}{2}F_{\rho\sigma} \pm T_{\rho\sigma})$$

$$-(\gamma/4N)a^4 \sum_{\square} \sigma_{ijkl}^{\mu\nu}\sigma_{ijkl}^{\rho\sigma} F_{\mu\nu} F_{\rho\sigma} \qquad (20)$$

This expression shows that $F_{\mu\nu}$ and $T_{\mu\nu}$ decouple as $a \to 0$. Hence, $T_{\mu\nu}$ appears only with a term in $T_{\mu\nu}^2$ in the action, to this order. The next term is of order a^6 and contains derivatives. Thus, the kinetic part of $T_{\mu\nu}$ is of order a^2 leading to a mass $\sim 1/a$. Thus as $a \to 0$, $T_{\mu\nu}$ gets an infinite mass and does not propagate However, for finite a, $T_{\mu\nu}$ plays a part in the regularization procedure. As is pointed out in Ref.[45] its presence is expected to affect the Λ parameter of the theory which turns out to be quite different from the corresponding hypercubical lattice.

Finally, we evaluate the unoriented sums in (20) as $a \to 0$. using eq.(7) for the volume per lattice site, we have

$$\sum_{\Delta} = 2\sum_{\text{sites}} 2 \sum_{i<j<k} \to 4\sum_{i<j<k} a^{-d(d+1)^{-1/2}} \int d^dx \qquad (21)$$

where the first factor of 2 sums over orientations and the second accounts for the two triangles per orientation. We write

$$\sigma_{ijk}^{\mu\nu}\sigma_{ijk}^{\rho\sigma} = A(\delta^{\mu\rho}\delta^{\nu\sigma} - \delta^{\mu\sigma}\delta^{\nu\rho}) \qquad (22)$$

and contract with $\delta^{\mu\rho}\delta^{\nu\sigma}$ to get

$$A(d^2-d) = (\sigma_{ijk})^2 = (1/9)\ (\epsilon_{ij}{}^{\mu}\epsilon_{jk}{}^{\nu}+\epsilon_{jk}{}^{\mu}\epsilon_{ki}{}^{\nu}+\epsilon_{ki}{}^{\mu}\epsilon_{ij}{}^{\nu})^2$$

$$= [d(d+1)(d-1)/54][3\vec{\epsilon}_{ij}{}^2 \cdot \vec{\epsilon}_{jk}{}^2 + 6(\vec{\epsilon}_{ij} \cdot \vec{\epsilon}_{jk})^2]$$

From (3) we get $\vec{\epsilon}_{ij}{}^2 = 2$ and $\vec{\epsilon}_{ij} \cdot \vec{\epsilon}_{jk} = -1$. Hence

$$A = (d+1)/3 \qquad (23)$$

Similarly for the squares

$$\sum_{\square} = 2 \sum_{\text{sites}} 1 \sum_{\substack{i<j \\ k<l \\ i<k \\ i,j,k,l \text{ all different}}} = 2 \sum_{\substack{\square \\ \text{orient/ns}}} a^{-d(d+1)^{-1/2}} \int d^d x \qquad (24)$$

We have as before

$$\sigma_{ijkl}^{\mu\nu}\sigma_{ijkl}^{\rho\sigma} = A'\ (\delta^{\mu\nu}\delta^{\rho\sigma} - \delta^{\mu\rho}\delta^{\nu\sigma}) \qquad (25)$$

with $$A' = (d+1)(d+2)/4 \qquad (26)$$

Collecting everything, we get for the continuum limit action

$$S = -(\beta/3\mathcal{N})a^{4-d}(d+1)^{1/2}\int d^dx\ 2\ tr(\tfrac{1}{2}\mathcal{F}_{\mu\nu}\pm\mathcal{T}_{\mu\nu})^2$$

$$-(\gamma/8\mathcal{N})a^{4-d}(d+1)^{1/2}(d-2)\int d^dx\ 2\ tr(\mathcal{F}_{\mu\nu})^2 \qquad (27)$$

Specializing to 4-dimensional U(1) theory with $\mathcal{N}=1$ and $\mathcal{F}_{\mu\nu}=F_{\mu\nu}=\partial_\mu A_\nu-\partial_\nu A_\mu$, we find for the $F_{\mu\nu}$ part of the action :

$$S = \frac{2\sqrt{5}}{3}(\beta+3\gamma)\int d^dx\ \tfrac{1}{4}F_{\mu\nu}{}^2 \qquad (28)$$

Thus the bare coupling constant g_0 is identified with

$$\frac{1}{g_0{}^2} = \frac{2\sqrt{5}}{3}(\beta+3\gamma) \qquad (29)$$

This result shows that the effect of the square term in the action can be accounted for by replacing the coupling β by an effective coupling $\beta+3\gamma$.

4. MONTE-CARLO RESULTS

In this section we report on the results of a Monte-Carlo investigation of the U(1) simplicial lattice model with the Wilson action. The object of this analysis was first of all to ensure that known U(1) results are reproduced in accordance with the expectation that long-distance, continuum physics should not depend on the particular details of the lattice, and secondly to determine what computational advantages, if any, should be afforded in this model.

In Table 2 we summarize some geometrical properties of the simplicial lattice which are interesting from a computational point of view. These follow easily from the description of the simplicial lattice geometry, given in Sec.2. We expect from that table that a full simplicial lattice iteration will be slower than the corresponding hypercubic lattice iteration by a factor of $\sqrt{5}$. However this disadvantage should be compensated by two factors. First, thermalization is achieved much more rapidly and second, we need fewer data points for results of comparable accuracy. Both these expectations are borne out in the subsequent calculations.

The program was written in FORTRAN 77 and was designed for maximum portability (ie with a minimum number of non-standard features). The calculations were carried out partly on the University of London Computer Centre machines (CDC7600 and Cray 1-S) and partly on the VAX 11/780 at the Royal Holloway College Computer Centre. In its original version, described in Ref.[46],

it was designed for a four dimensional simulation with a general SU(N) or U(N) group. In that version we have used the modified Metropolis algorithm for updating, as described in Section I3. The performance of that program was improved by two features: a weighting of the random matrices towards the identity for weak couplings and a subroutine RENORM which was referenced periodically to perform a Gram-Shmidt orthogonalization on the link matrices thus restoring them to the correct group symmetry. However, for the U(1) application we have found it profitable to modify the program on two counts. Firstly, we have used a heat bath algorithm, also described in Section I3. Secondly the group elements were stored in variables rather than 1x1 arrays.

The program measures expectation values of the elementary plaquette operator (triangles) as well as of twelve other types of triangular and rectangular Wilson loops (Fig.3). We have chosen to use periodic boundary conditions (they are the simplest to program), such that for a lattice of linear dimension L the points x_i and y_i are identified so that $x_i - y_i = 0$ (modulo L). However this method should not be adopted in calculations where the size of the lattice is allowed to vary independently in different directions (eg in finite temperature calculations). In such cases other prescriptions have to be used instead.

For the main calculation we have used a lattice with six sites per dimension (12960 links). We have simulated with the Wilson action containing a single 'triangle' term since, as was

shown in the previous section, inclusion of the square plaquettes in the action merely amounts to a trivial renormalization of the coupling parameter. The action is thus

$$S[U] = \beta \sum_{\Delta} S_{\Delta} \tag{30}$$

where β is proportional to the inverse coupling constant squared and

$$S_{\Delta} = 1 - Re U_{\Delta} \tag{31}$$

where U_{Δ} are products of U(1) elements taken round an elementary triangle on the lattice. Each link (ij) is thus associated with an angle θ_{ij}, in the range from zero to 2π :

$$U_{ij} = \exp(i\theta_{ij}) \tag{32}$$

and

$$U_{ji} = \exp(-i\theta_{ij}) \tag{33}$$

We define the partition function by

$$Z(\beta) = \int \prod_{i,j} [DU_{ij}] \exp(-S[U]) \tag{34}$$

where the U(1) normalized Haar measure is given by

$$DU_{ij} = d\theta_{ij}/2\pi \tag{35}$$

As mentioned in Chapter I, expectation values of operators W(C) defined on closed contours C are defined as

$$\langle W(C)\rangle = Z^{-1} \int \prod_{i,j} [DU_{ij}] W \exp(-S[U]) \tag{36}$$

They can be replaced by configurational averages over Monte-Carlo cycles

$$\langle W(C)\rangle \underset{N\to\infty}{\to} N^{-1} \sum_{n} W_n(C)$$

where W_n is the result of the n^{th} measurement, averaged over all embeddings of the given operator on the lattice.

In Fig.4 we show the evolution of the average plaquette operator with the number of Monte-Carlo cycles. It can be seen that in the region $\beta<0.7$ and $\beta>1.0$ the lattice thermalizes very quickly, and a number of iterations of the order of 10 was enough to bring about thermal equilibrium. In this region we have carried out 50 iterations and averaged over the last thirty. However in the region $0.70<\beta<1.00$ it was found necessary to perform 500 iterations and average over the last 300. In order to reduce correlations between successive measurements we have discarded

every second configuration. With these precautions, the statistical fluctuations on our measurements were smaller than the size of the dots in all the figures, even for the larger loops. We have also performed an error analysis on our data on the basis of ref.[32] which indicated no significant increase in the statistical errors when correlating between successive measurements were taken into account.

In Fig.5 we show the variation of the average action per plaquette with respect to β . The quantity we plot is defined by

$$< E_\Delta > = 1 - < W_\Delta > / N_\Delta \qquad (38)$$

where $<W_\Delta>$ is the expectation value of the triangular plaquette operator and N_Δ is the number of triangles on the lattice. The shape of the curve is qualitatively very similar to similar results obtained with the hypercubic lattice with a sharp change in slope around $\beta = 1.0$ suggesting a phase transition. The data are also in very good agreement with a low-order strong coupling expansion

$$< E_\Delta > = 1 - \beta/2 + \beta^3/16 - \beta^4/120 + O(\beta^7) \qquad (39)$$

and with the weak coupling (large β) result

$$< E_\Delta > = 1/4\beta + O(\beta^{-2}) \qquad (40)$$

Expressions (39) and (40) are also plotted in Fig.5.

In Fig.6 we show the triangular Wilson loops along with their expected strong coupling behaviour to leading order

$$< W(C) > = (\tfrac{1}{2}\beta)^{\text{area}} + \ldots \qquad (41)$$

where the area of the loop is expressed in lattice units. The numbering scheme for our loops is shown in Fig.3. In order to extract the area law behaviour we consider appropriate ratios of loops. For example the loop W(I,J) shown numbered 13 in Fig.3, has an area $(b^2\sqrt{3}/4)(I^2+4IJ+J^2)$ and a perimeter $3b(I+J)$, where b is the nearest neighbour distance on the simplicial lattice. As explained in Chapter I, we assume a Wilson loop behaviour

$$< W(C) > \sim e^{K.\text{area} + \lambda.\text{perimeter}} \qquad (42)$$

where the coefficient K is the string tension. K can therefore be extracted from

$$K = -\frac{2}{3\sqrt{3}} \ln\left[\frac{W(I+1,I+1)\, W(I,I-1)}{W(I,I)\, W(I,I-1)}\right] \qquad (43)$$

and from similar Wilson loop ratios where the perimeter terms cancel. With the triangular loops at our disposal (types 1,2,3,4,6,9,13) we construct the ratios

$$\chi_1^{\Delta} = (2\sqrt{3}/3)\ \ln(W_4^{\Delta}/W_6^{\Delta})$$

$$\chi_2^{\Delta} = (2\sqrt{3}/3)\ \ln(W_1^{\Delta}W_6^{\Delta}/W_2^{\Delta}W_3^{\Delta})$$

$$\chi_3^{\Delta} = (\sqrt{3}/3)\ \ln(W_9^{\Delta}/W_{13}^{\Delta}) \qquad (44)$$

$$\chi_4^{\Delta} = (2\sqrt{3}/3)\ \ln(W_4^{\Delta}W_4^{\Delta}/W_1^{\Delta}W_9^{\Delta})$$

These results are plotted in Fig.7. Also in Fig.7 we plot the strong-coupling expression for K^{Δ} given by

$$K^{\Delta} = -(4/\sqrt{3})(\ln\beta + 2\beta^2 - 31\beta^4/16 + O(\beta^6)) \qquad (45)$$

The rapid decrease in the string tension at weak couplings would suggest that in the infinite volume limit the coefficients of eq.(44) might vanish altogether, suggesting a deconfining phase transition. Similar results are obtained with the square Wilson loops (types 1,2,3,4,6,9 in Fig.3). These are shown in Fig.8 with the leading order strong coupling behaviour

$$\langle E \rangle = 2(\tfrac{1}{4}\beta)^4 + O(\beta^6) \qquad (46)$$

The area law behaviour for the square loops is extracted from the ratios

$$\chi 1 = \ln(W_3^{\square} / W_4^{\square})$$
$$\chi 2 = \ln(W_2^{\square} W_6^{\square} / W_3^{\square} W_4^{\square}) \qquad (47)$$

where, as before, perimeter terms cancel. These results are shown in Fig.9 . The leading order strong coupling expansions for K is given by

$$K = -4 \ln\beta \qquad (48)$$

The similarity of the graphs for the area law coefficients in Figs. 7 and 9 suggests that the lattice is invariant in the different two-planes containing square and triangular Wilson loops.

In order to compute various quantities of interest in the continuum limit and to compare them with the equivalent ones for a hypercubic lattice, we have performed a finite size scaling analysis on our data. Bearing in mind the computing resources available we have worked on lattices of size 4^4,5^4 and 6^4. Fig.10 shows the variation of the specific heat with beta at the above sizes. We have defined the specific heat by

$$C = \partial\langle E_\Delta\rangle/\partial T = -\beta^2 \partial\langle E_\Delta\rangle/\partial\beta = -\beta^2[\langle E_\Delta^2\rangle - \langle E_\Delta\rangle^2] \qquad (49)$$

It is evident from Fig.10 that within our data, the position of the maximum in the specific heat does not vary appreciably with increasing lattice size. However, because of the difficulty in locating the exact position of the peaks we have chosen to do a quantitative analysis on the average plaquette action.

The results for sizes 4^4, 5^4 and 6^4 are shown in Fig.12. We have taken 12 data points in the range $0.90 \leq \beta \leq 1.0$. For each of the 4^4 points we have performed 5000 iterations discarding the first 3000, for the 5^4 points we have done 4000 iterations discarding the first 2000 and for the 6^4 points we have done 3000 iterations and discarded the first 1000.

The basic assumption in the finite size scaling analysis is that in a finite system near a second order phase transition the correlation length becomes of the order of the size of the system. Of course, in an infinite system the correlation length would diverge as

$$\xi \sim |\beta-\beta_c|^{-\nu} \tag{50}$$

where β_c is the critical temperature of the infinite system and ν is a positive critical exponent. For a finite system of size L we therefore assume

$$\xi_L = Ls(x) \tag{51}$$

where $s(x)$ is a scaling function satisfying

$$s(0) = 1 \qquad \text{and} \qquad \lim_{x\to\infty} s(x) = x^{-\nu} \tag{52}$$

Hence, we define

$$x = |\beta-\beta_L|\ L^{1/\nu} \tag{53}$$

to satisfy eq.(50). Now from the scaling of the free energy $F\sim L^{-d}s(x)^{-d}$, we find

$$E(\beta,L) = dF(\beta,L)/d\beta = A_0 + A_1|\beta-\beta_L|^{\rho}\text{sign}(\beta-\beta_L) \tag{54}$$

where $\rho=\nu d-1$ and A_0, A_1, ρ and β_L are the fitting parameters to be determined. A least squares fit to the 6^4 data shown in Fig. 11 produced the following values for the parameters:

$$A_0 = 0.64338 \pm 0.00085 \tag{55}$$

$$A_1 = 0.25620 \pm 0.00073 \tag{56}$$

$$\rho = 0.39492 \pm 0.00123 \tag{57}$$

$$\beta_L = 0.95142 \pm 0.00049 \tag{58}$$

with similar results for the 5^4 and 4^4 given in Table 3. Eq.(57) gives for the correlation length critical exponent

$$\nu = 0.34873 \pm 0.0003 \qquad (59)$$

in very good agreement with similar analyses, refs.[17] and [19]. Now, from equations (52) and (53) it can be shown that, for large L

$$\beta_c - \beta_L = cL^{-1/\nu} \qquad (60)$$

where c is a constant and β_c is the critical temperature of the infinite lattice. A least squares fit to eq.(60) with the data of Table 3 yields

$$\beta_c = 0.9517 \pm 0.0082 \qquad (61)$$

This is smaller than other determinations, evidently due to the particular nature of the simplicial lattice.

5. SUMMARY AND CONCLUSIONS

In this chapter we have examined some aspects of the U(1) lattice gauge theory formulated on the simplicial lattice. We have shown that this lattice has the correct continuum limit and presented Monte-Carlo results for the average plaquette and various types of Wilson loops which compare well with low order strong coupling expansions. The string tension results in the two-planes containing triangular and square Wilson loops and show some evidence for improved rotational invariance.

In accordance with similar investigations on the hypercubic lattice, the simplicial lattice with the Wilson action shows evidence of undergoing a second order phase transition at approximately $\beta = 0.95$ and with an associated correlation length critical exponent $\nu \sim 1/3$. The more closely packed nature of this lattice implies that fluctuations in the local variables play a less important role and the Coulomb-type phase sets in at lower values of the coupling, corresponding to coarser lattices. As a consequence, the specific heat results are smoother, with less variation in the position of the peaks as a function of the lattice size. Similarly, the average plaquette data are more regular and accurate, enabling good fits to continuum limit parameters to be obtained from relatively small lattices.

TABLES

TABLE 1

Comparison of hypercubic and simplicial lattice geometries in d-dimensional space.

	Hypercubic	Simplicial
Volume per site	a^d	$a^d(d+1)^{1/2}$
Degrees of freedom per site	d	$\frac{1}{2}d(d+1)$
Triangular plaquettes per site	-	$d(d^2-1)/3$
Square plaquettes per site	$\frac{1}{2}d(d-1)$	$d(d^2+1)(d^2-2)/8$

TABLE 2

Estimation of the relative times for a Monte-Carlo interation for hypercubical and simplicial lattices.

Number of matrix multiplications needed	Hypercubic	Simplicial
per link	12	6
per site	48	60
per volume expressed in lattice units	48	48

TABLE 3

Estimated values of parameters and their errors to the fits to eq.(54) of the text for various lattice sizes

Lattice size	βL	ρ
4^4	0.9511 ± 0.0001	0.5620 ± 0.0007
5^4	0.9514 ± 0.0000	0.4479 ± 0.0009
6^4	0.9514 ± 0.0001	0.3949 ± 0.0003

FIGURE CAPTIONS

Fig. 1a: Elementary triangles in the lattice in the section $(\vec{e}_{ij}, \vec{e}_{jk})$ with i, j, k all different.

Fig.1b: Elementary squares in the lattice exist in the planes $(\vec{e}_{ij}, \vec{e}_{kl})$ with i, j, k, l all different.

Fig.2: Evaluation of the gauge field resultant at the centre X of the triangle. The inverted triangle also exists. It corresponds to the lower sign in the equations of Sec.II3.

Fig.3: Triangular and square Wilson loops calculated in the program with their numbering scheme.

Fig.4: The evolution of the average plaquette operator with the number of Monte-Carlo sweeps for various values of β .

Fig.5: Variation of the average triangular plaquette as a function of β . The solid lines show the corresponding strong and weak coupling expansions (see text, eqs.(39) and (40)).

Fig.6: Variation of various triangular Wilson loops as functions of β . The solid lines show the corresponding strong coupling expansions (area law). The numbering scheme is as in Fig.3.

Fig.7: The string tension in the triangular planes as a function of β . Also shown in solid lines is the strong coupling expansion obtained to various orders in β. The χ_i's correspond to eq.(44) in the text.

Fig.8: Variation of the square Wilson loops as functions of β . The solid line shows the leading order strong coupling behaviour for the square plaquette. The numbering scheme is shown in Fig.3.

Fig.9: The string tension in the planes containing square loops as a function of β . The solid line represents the leading order strong coupling behaviour. The χ_i's correspond to eq.(47) in the text.

Fig.10: The specific heat $C=\partial\langle E\rangle/\partial T$ for the simplicial lattice as a function of β and the lattice size. The data for the 4^4, 5^4 and 6^4 lattices are represented by diamonds,crosses and open circles respectively.

Fig.11: Variation of the average triangul;ar plaquette as a function of β and the latrtice size for lattices of 4^4, 5^4 and 6^4 sites. The solid curve shows a fit (eq.(54) of the text) to the 6^4 data with the parameters shown in eqs. (55)-(58) in the text. The symbopls are as in Fig. 11.

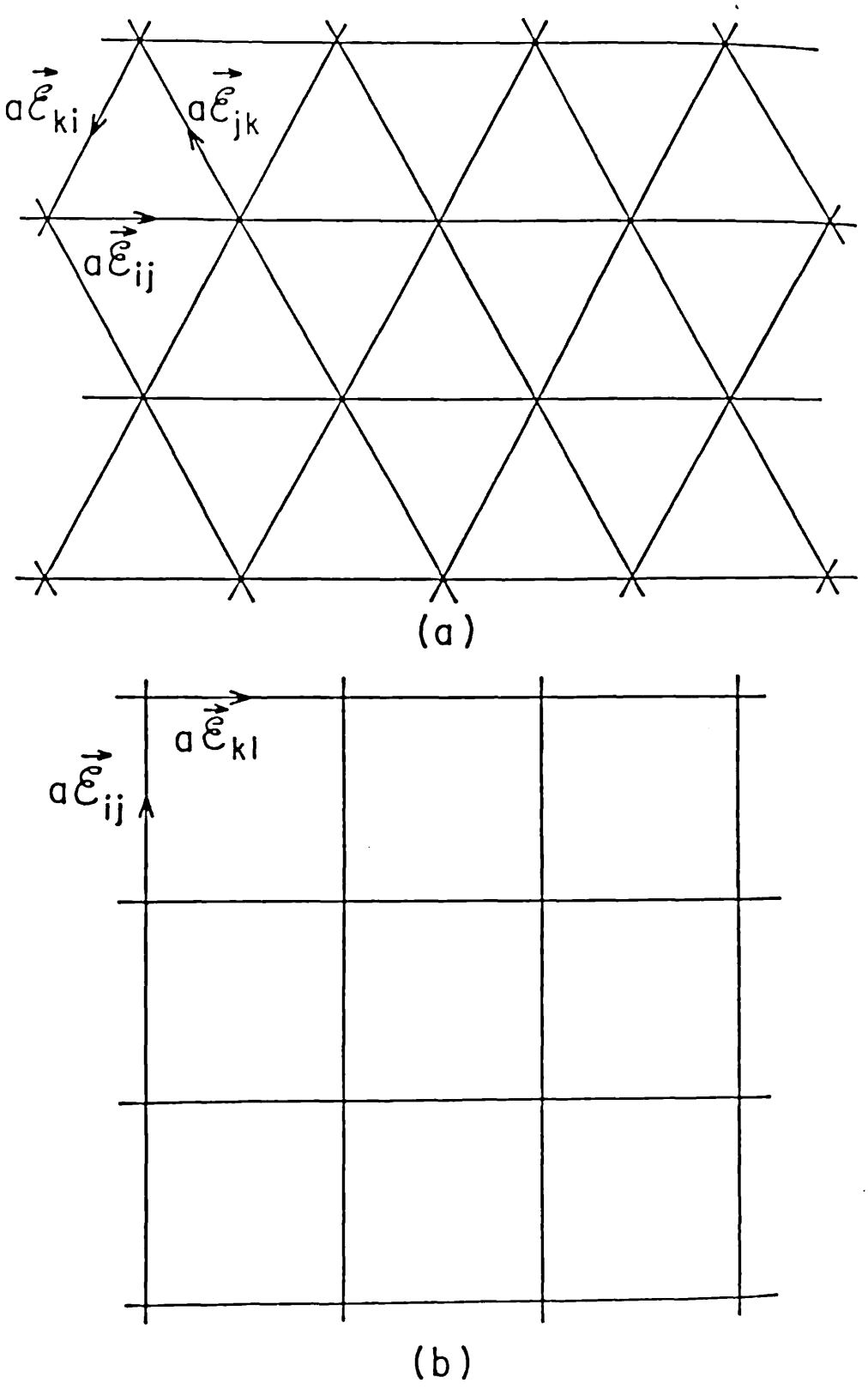
$a\vec{\varepsilon}_{ki}$
$a\vec{\varepsilon}_{jk}$
$a\vec{\varepsilon}_{ij}$
(a)
$a\vec{\varepsilon}_{kl}$
$a\vec{\varepsilon}_{ij}$
(b)

Fig. 1

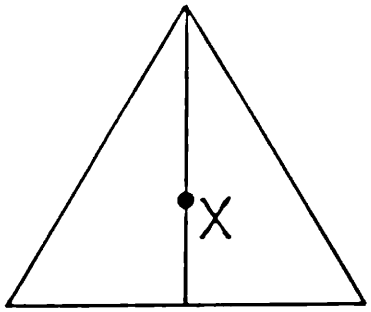

Fig. 2

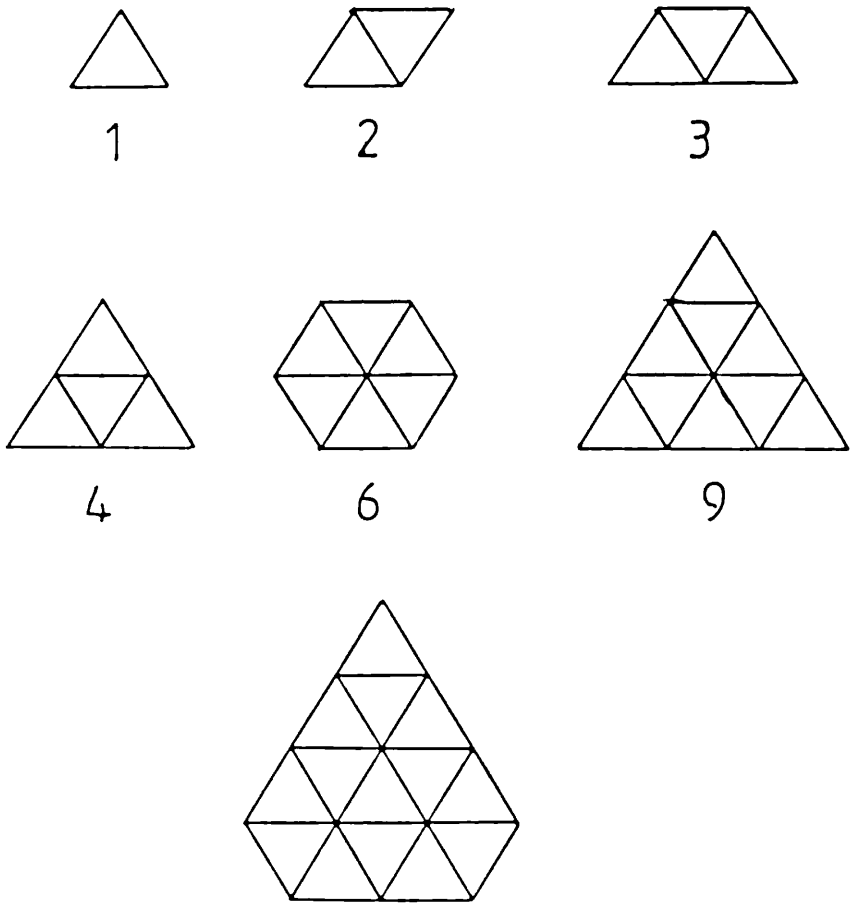

(a)

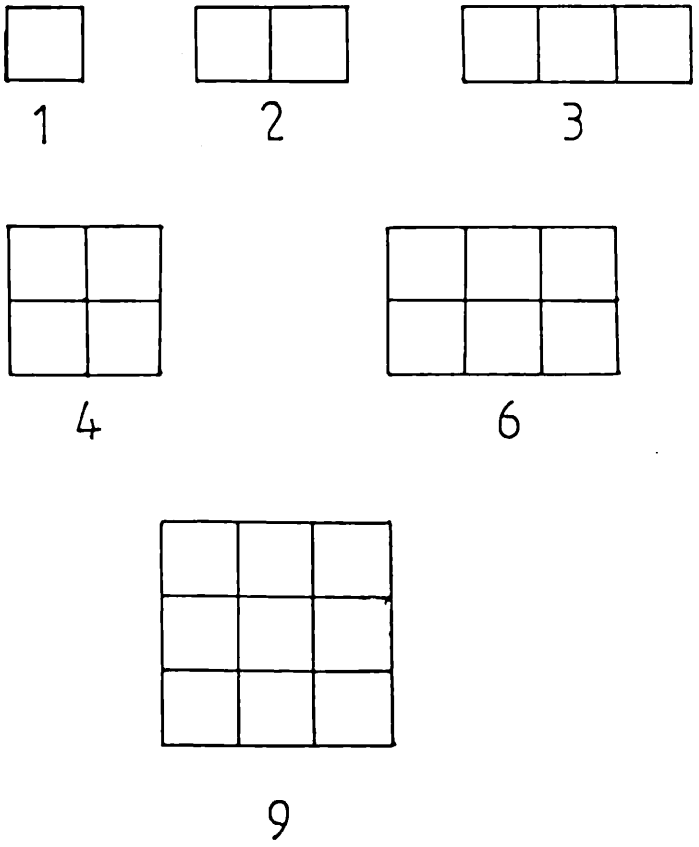

(b)

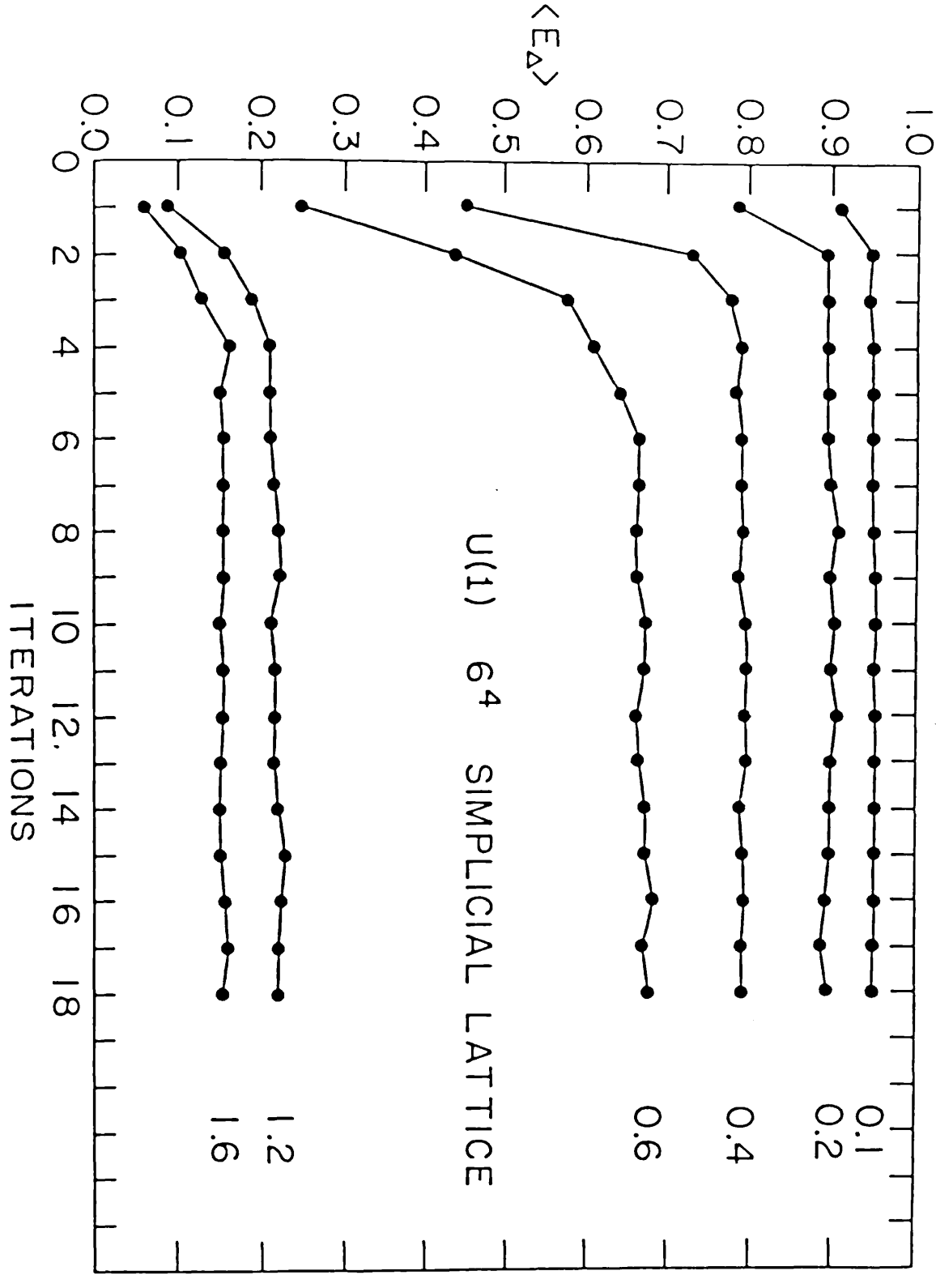
1.0
0.9
0.8
0.7
0.6
0.5
0.4
0.3
0.2
0.1
0.0
<EΔ>
0
2
4
6
8
10
12
14
16
18
ITERATIONS
U(1) 6⁴ SIMPLICIAL LATTICE
0.1
0.2
0.4
0.6
1.2
1.6

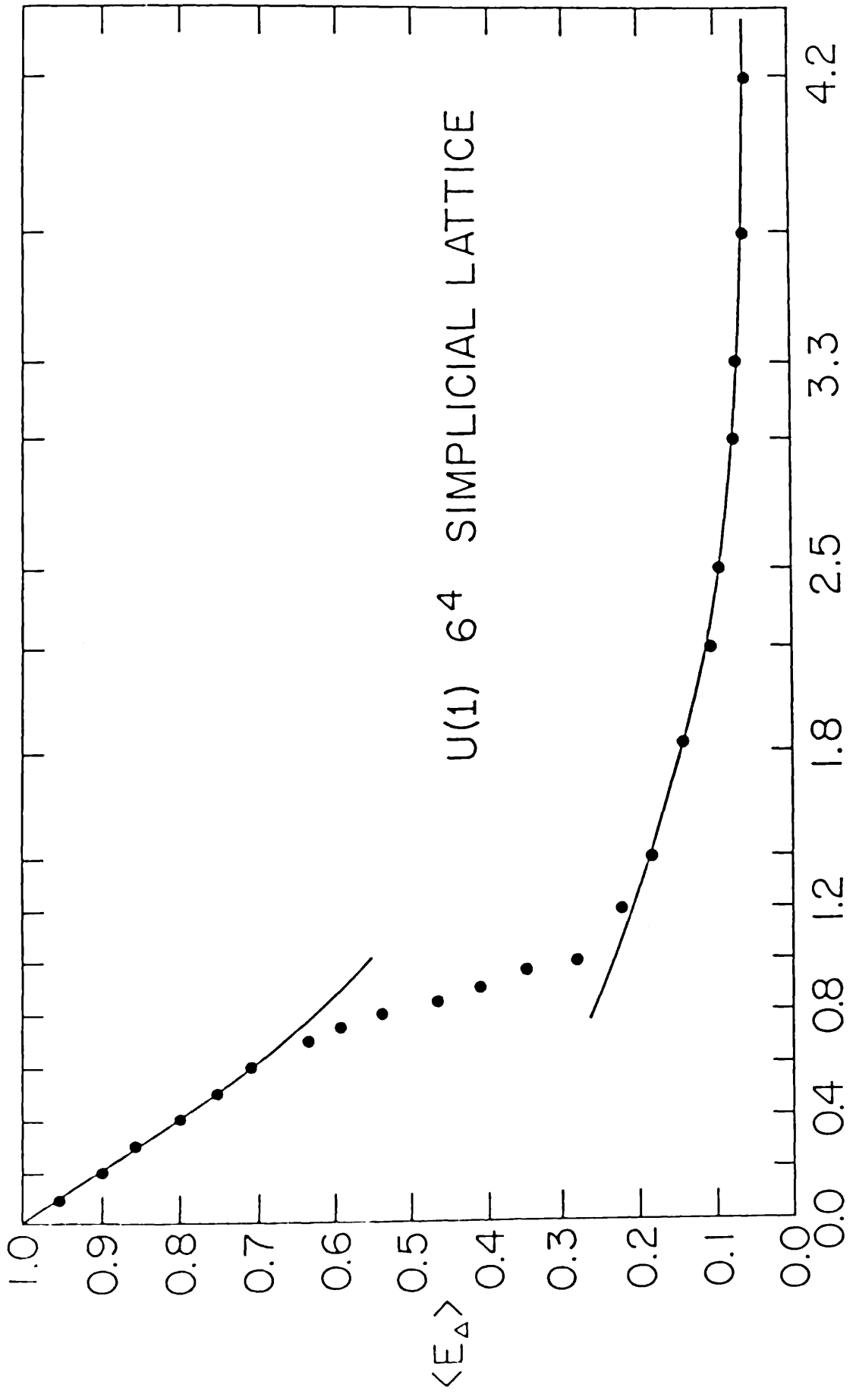
U(1) 6^4 SIMPLICIAL LATTICE
$\langle E_\Delta \rangle$
β
1.0
0.9
0.8
0.7
0.6
0.5
0.4
0.3
0.2
0.1
0.0
0.0
0.4
0.8
1.2
1.8
2.5
3.3
4.2

Fig. 5

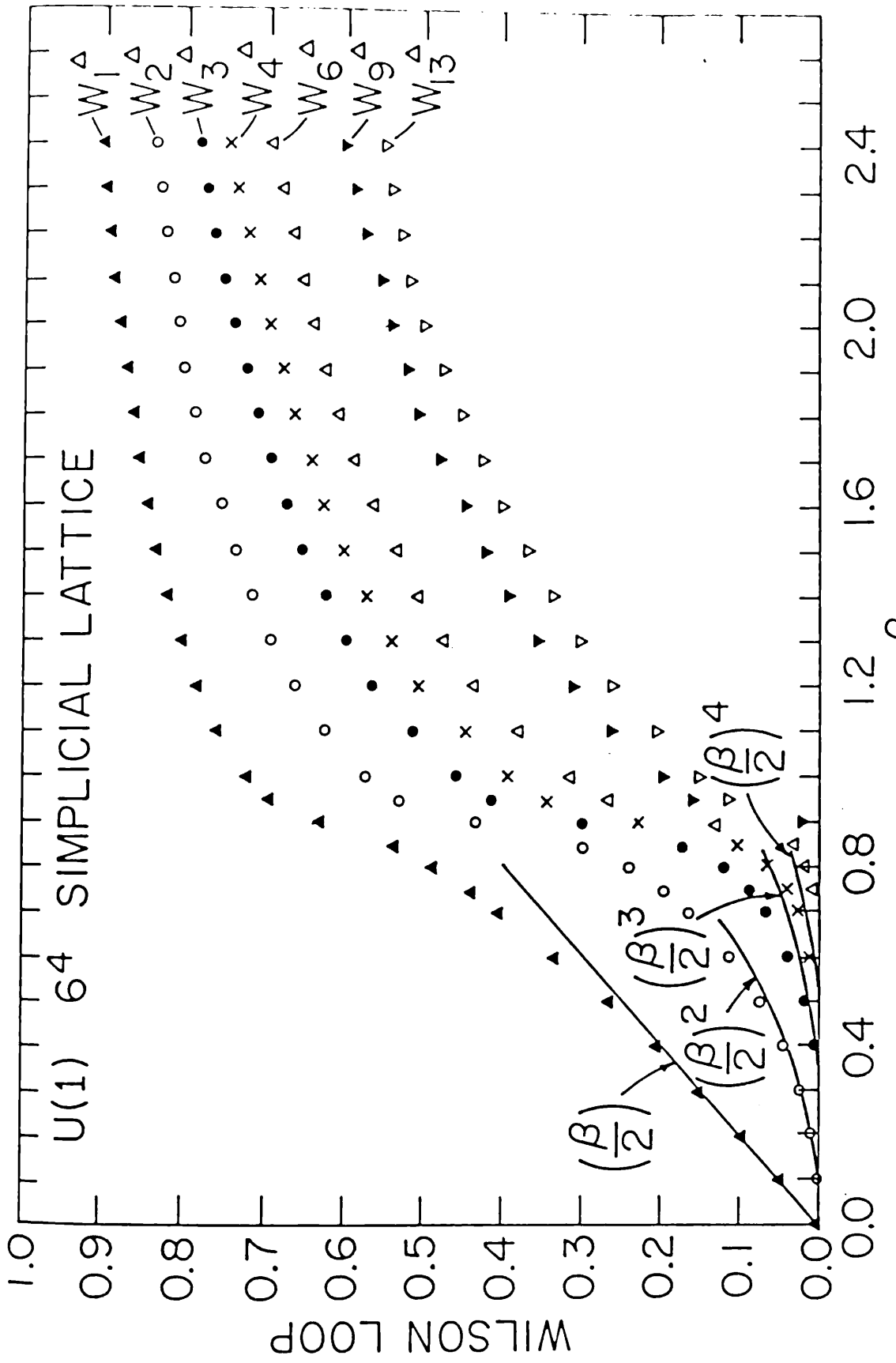
U(1) 6^4 SIMPLICIAL LATTICE
WILSON LOOP
β
W_1
W_2
W_3
W_4
W_6
W_9
W_{13}
$(\beta/2)$
$(\beta/2)^2$
$(\beta/2)^3$
$(\beta/2)^4$
0.0
0.1
0.2
0.3
0.4
0.5
0.6
0.7
0.8
0.9
1.0
0.0
0.4
0.8
1.2
1.6
2.0
2.4

Fig. 6

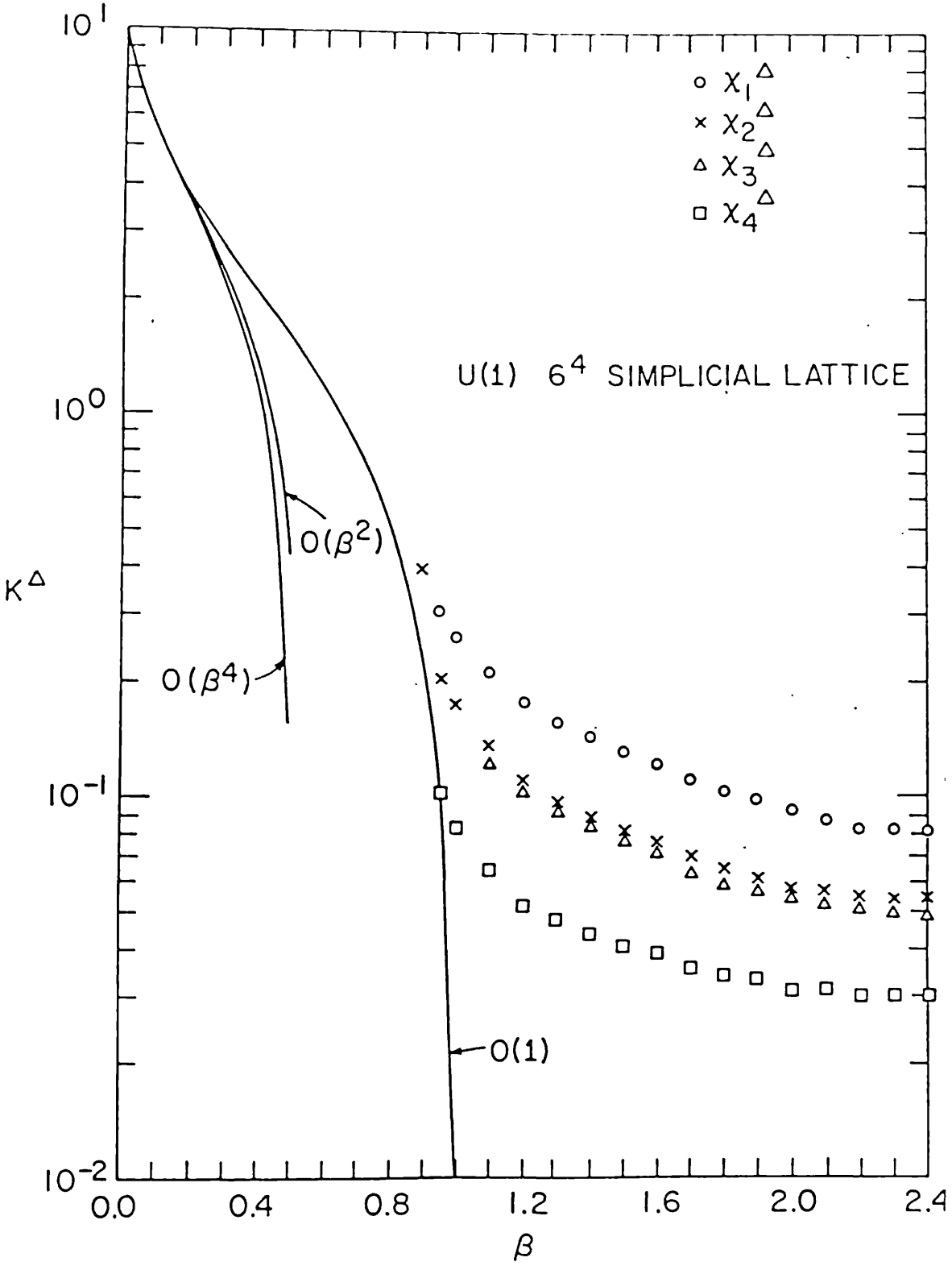
10^1
10^0
10^{-1}
10^{-2}
K^Δ
χ_1^Δ
χ_2^Δ
χ_3^Δ
χ_4^Δ
U(1) 6^4 SIMPLICIAL LATTICE
$O(\beta^2)$
$O(\beta^4)$
O(1)
0.0
0.4
0.8
1.2
1.6
2.0
2.4
β

Fig. 7

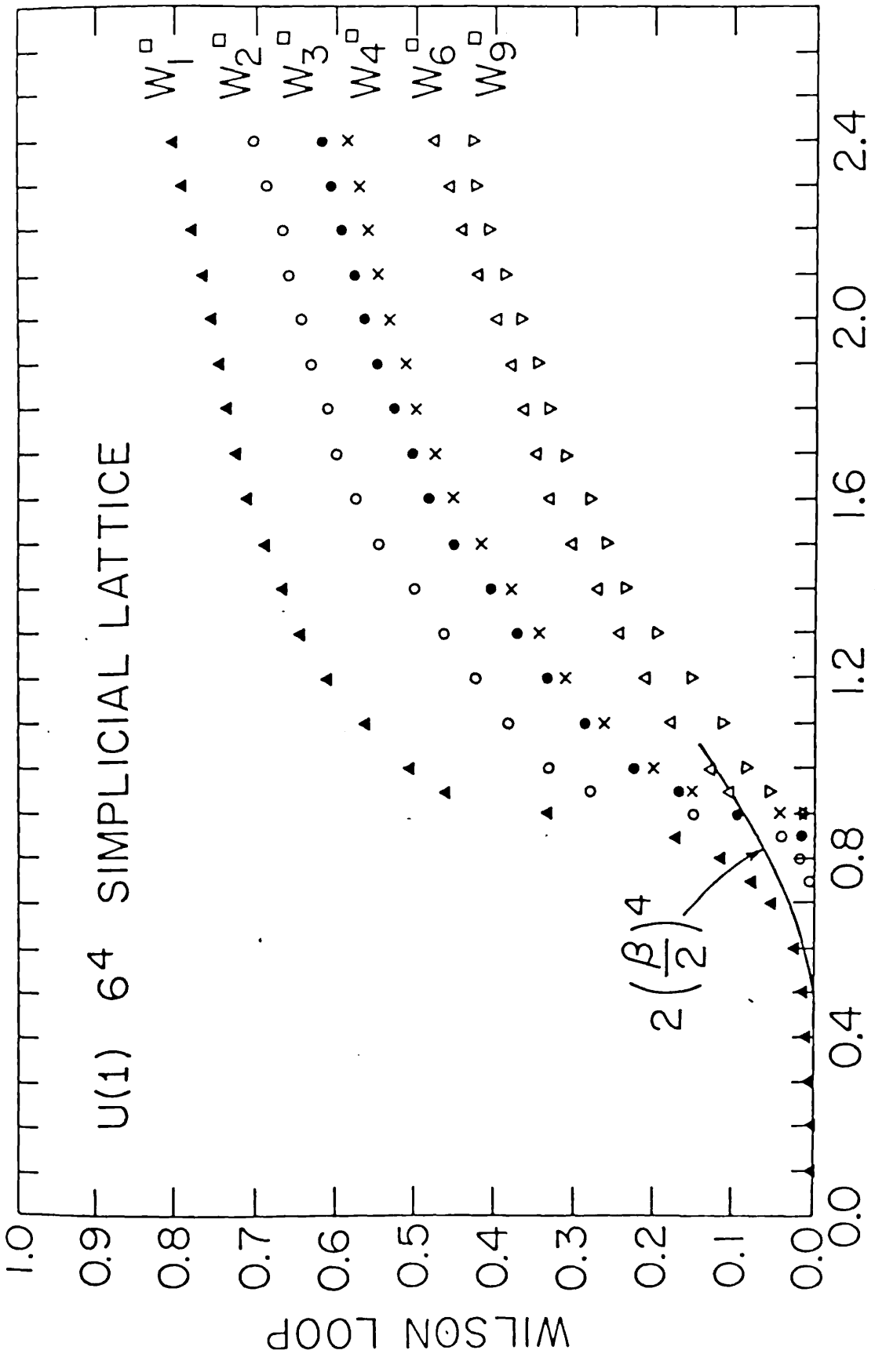
U(1) 6^4 SIMPLICIAL LATTICE
W_1
W_2
W_3
W_4
W_6
W_9
$2\left(\frac{\beta}{2}\right)^4$
WILSON LOOP
β
0.0
0.1
0.2
0.3
0.4
0.5
0.6
0.7
0.8
0.9
1.0
0.0
0.4
0.8
1.2
1.6
2.0
2.4

Fig. 8

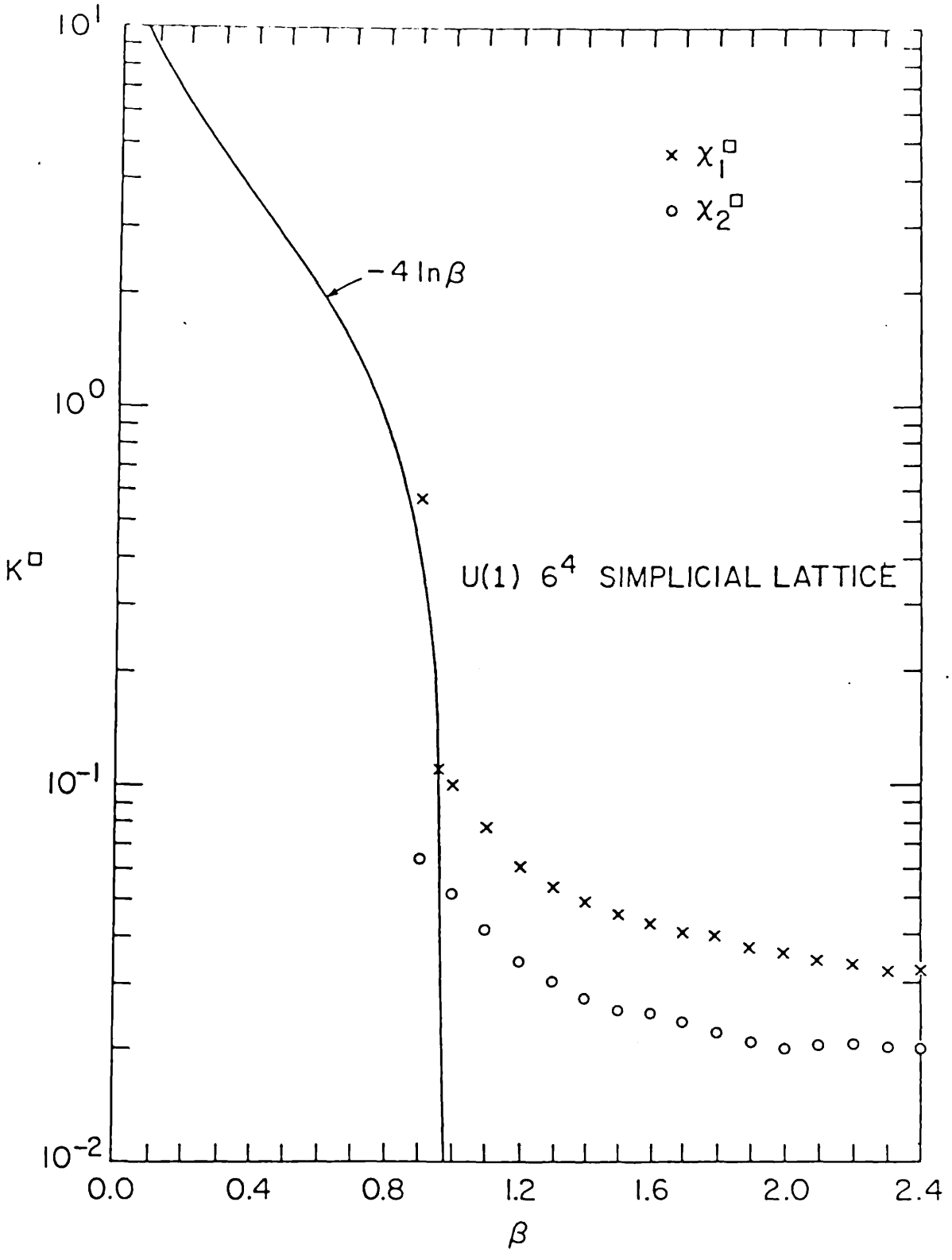
10^1
10^0
10^{-1}
10^{-2}
$K^{\square}$
$\times\ \chi_1^{\square}$
$\circ\ \chi_2^{\square}$
$-4\ln\beta$
U(1) 6^4 SIMPLICIAL LATTICE
0.0
0.4
0.8
1.2
1.6
2.0
2.4
β

Fig. 9

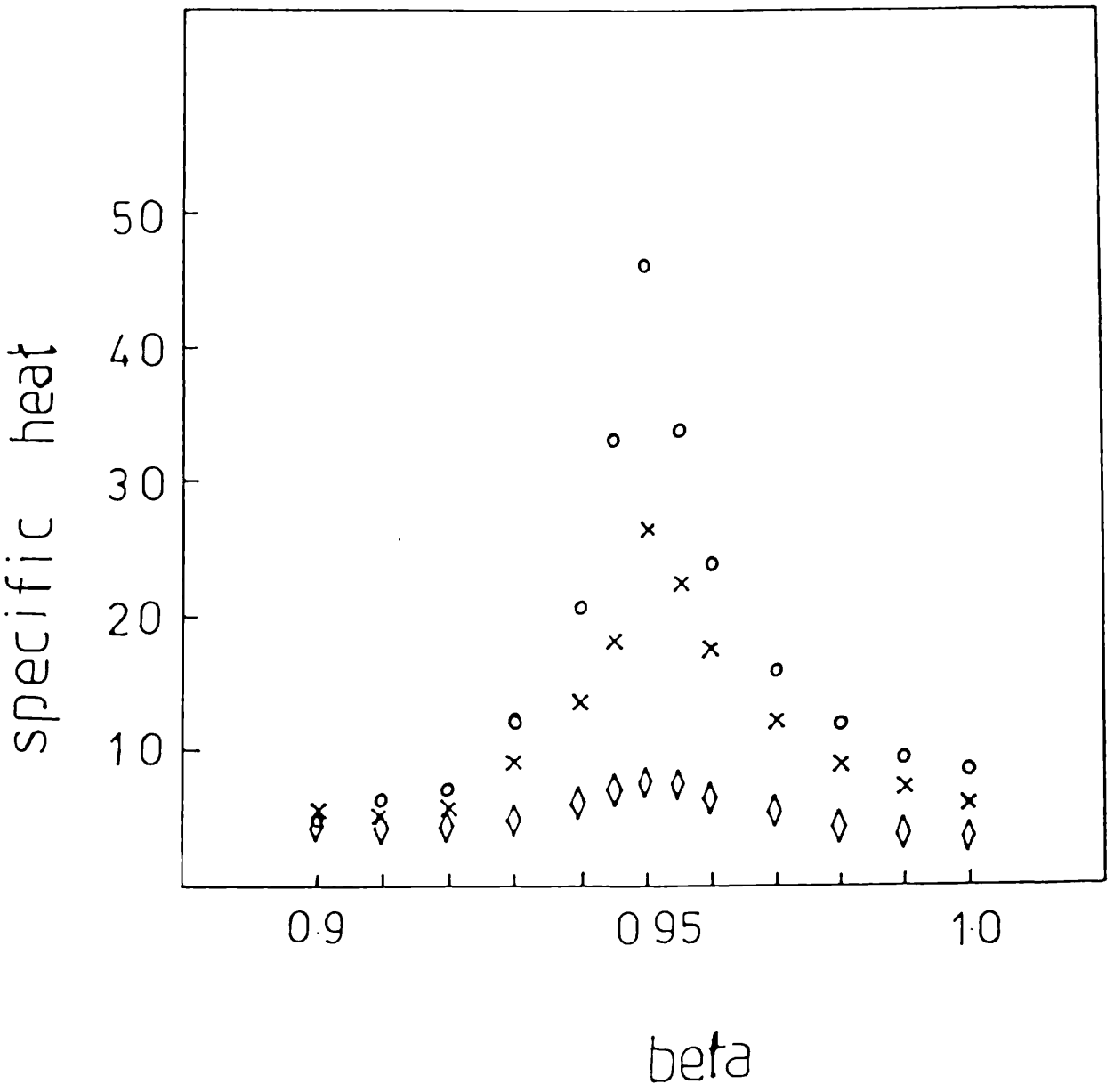

Fig. 10

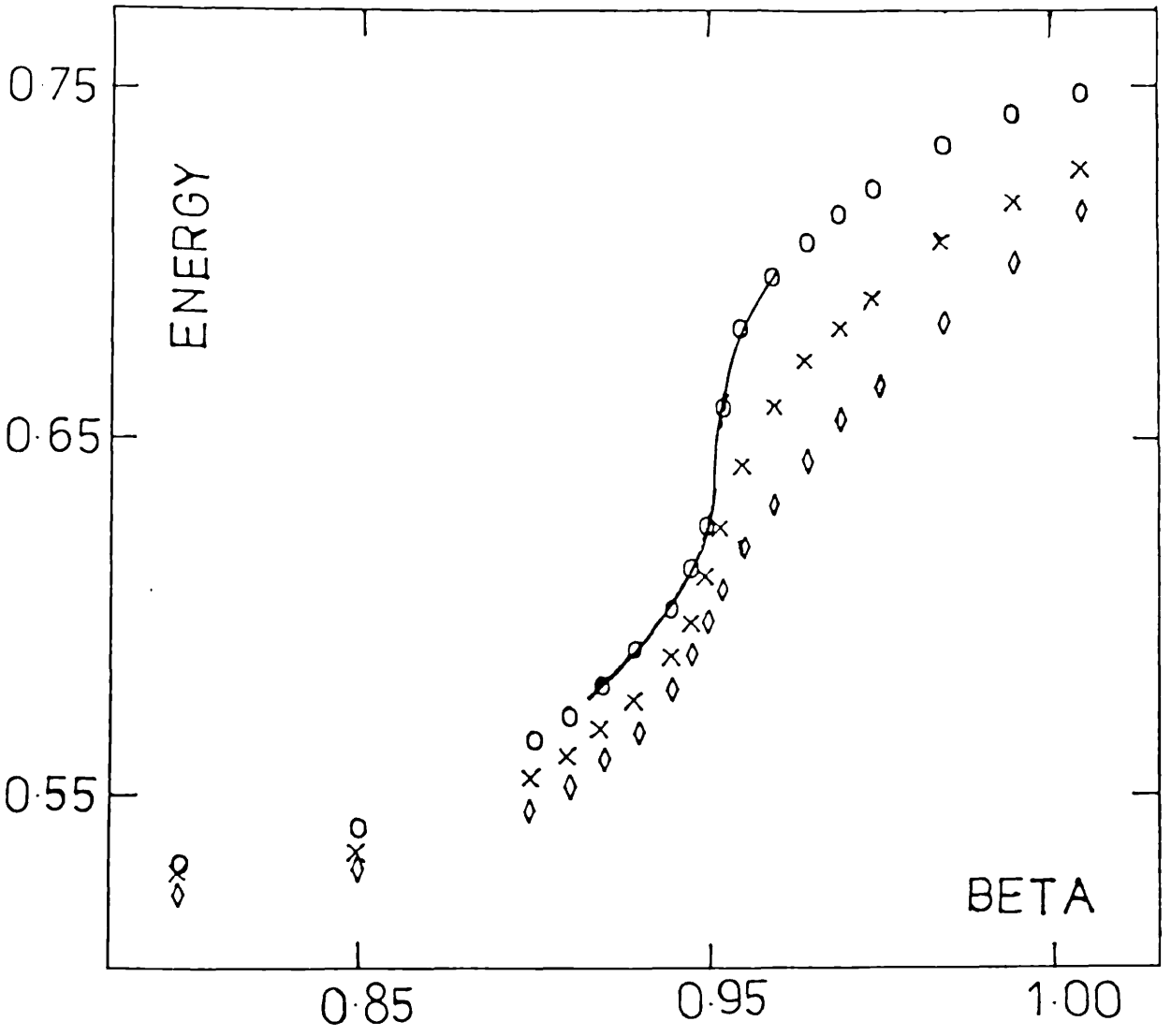

Fig. 11

CHAPTER III : THE RENORMALIZATION GROUP AND LATTICE QED.

1. Introduction

2. Background and formalism

   A. The Real Space Renormalization Group

   B. Monte-Carlo Renormalization Group Methods

3. Computational aspects

   A. General

   B. The Blocking Procedure

4. Results and discussion

   A. The Critical Exponents

   B. The Renormalized Parameters

5. Conclusions

1. INTRODUCTION

In Chapter II we have examined the U(1) lattice gauge theory on a simplicial lattice. We have been able to confirm the strong coupling expansions of that model and comment on certain aspects of the phase transition but we have been faced with the usual limitations of the Monte-Carlo approach: the long relaxation times near criticality and the finite-size rounding of critical singularities, both limit our ability to extract meaningful, continuum limit information from finite lattices.

In this Chapter we revert to a hypercubic lattice and adopt a subtler approach. We combine the Monte-Carlo technique with the ideas of the real space Renormalization Group. This approach is called Monte-Carlo Renormalization Group (MCRG). As will be seen, it allows to focus directly on the critical properties of our model while being systematically improvable and containing no uncontrolled approximations. In the following two subsections we describe briefly the background and formalism of the real space renormalization group and of MCRG. In Sec.3 we discuss some programming aspects. Sec.4A contains results from the critical exponents calculation. In Sec.4B we present the results on the calculation of the renormalized couplings. Finally in Sec.5 we present our conclusions and a discussion of possible future developments. As in the previous chapter we have employed a pure gauge action with no fermions. This work was carried out at Southampton University in collaboration with A. Burkitt and under the supervision of A. Hey.

2. BACKGROUND AND FORMALISM

2A. THE REAL SPACE RENORMALIZATION GROUP

In the renormalization group (RG) approach one aims to transform a given model with short range interactions into an equivalent one, in which the short-distance, irrelevant behaviour has been averaged out while the important, long-distance characteristics are unaffected [49].

The transformation is to be done in small steps which would hopefully be tractable. Thus, a sequence of actions is obtained, each with progressively fewer degrees of freedom. This procedure can be carried out in two ways

(i) Momentum space: A cut-off Λ in the theory's momenta is introduced. The RG scale factor is s. One integrates out the momenta in the range $\Lambda/s < p < \Lambda$ to find a new set of coupling parameters for the theory which would be functions of Λ . In this formulation one must also rescale the renormalized fields and momenta to fit the new description of the model.

(ii) Real space: The local degrees of freedom contained in a volume b^d in d-dimensional space, are grouped together into 'blocks' and each block is assigned a value according to some prespecified procedure (e.g. majority rule for discrete spin systems of average

over continuous variables). This method lends itself more readily to computer implementation and we shall concentrate on it for the rest of this Chapter.

Consider a general lattice gauge theory described by an action S. It is convenient to write the action in terms of a number of parameters (couplings) $\{K_a\}$ (a = 1, 2, ...). This is for two reasons: firstly, as was pointed out in the introduction there is no unique way of defining a lattice theory corresponding to a given continuum theory. Many Wilson loop operators of various shapes and sizes reduce to the standard $F_{\mu\nu} \cdot F_{\mu\nu}$ in the continuum limit. Secondly, starting with a single coupling, the RG transformation would generate a large (and evidently infinite) number of new couplings. So we write the most general starting lattice action as

$$S = \sum_a K_a S_a \qquad (1)$$

where the $\{S_a\}$ are all possible gauge invariant Wilson loop operators. The Euclidean partition function is

$$Z = \int [DU] e^{-S} \qquad (2)$$

where [DU] is the invariant group measure. We would like to 'thin out' the degrees of freedom by averaging over the short distance fluctuations. This is the RG blocking transformation and will

result in a new action, $S^{(1)}$ on a coarser lattice. The new action can then be described by a new set of renormalized couplings $\{K_a^{(1)}\}$ and operators $\{S_a^{(1)}\}$. Schematically we can write

$$S^{(1)} = R_b(S) = \sum_a K_a^{(1)} S_a^{(1)} \qquad (3)$$

where b is the RG scale factor. The RG transformation can be expressed in terms of a probability distribution $P(U^{(1)}, U)$ which 'translates' a system defined via the U's into one defined via the $U^{(1)}$'s:

$$\exp(-S^{(1)}) = \int [DU] P(U^{(1)}, U) e^{-S} \qquad (4)$$

$P(U^{(1)}, U)$ must be positive definite and satisfy

$$\int [DU^{(1)}] P(U^{(1)}, U) = 1 \qquad (5)$$

Eq.(5) ensures that the original and renormalized theories have the same partition function and hence the same long distance behaviour. A further, important requirement on $P(U^{(1)}, U)$ is that it must preserve the original theory's symmetries, in particular gauge invariance. In the particular RG transformation we have used in this work we have ensured that this requirement is indeed satisfied. This procedure can obviously be iterated:

$$S^{(n)} = R_b(S^{(n-1)}) = \sum_a K_a^{(n)} S_a^{(n)} \qquad (6)$$

Since successive applications of the RG transformation are designed to average out the short distance characteristics of the theory while leaving the long distance behaviour unaffected, the renormalized correlation length must be the same as the original. In units of the new lattice spacing we have

$$\xi' = \xi/b \qquad (7)$$

The sequence of actions $S^{(n)}$, each described by a set of couplings $\{K_a^{(n)};\ a = 1, 2, \ldots\}$ can be thought of as a trajectory in a multi-dimensional coupling constant space. The effect of the RG transformation therefore involves a mapping of an infinite dimensional space into itself. A fixed point in this space, S^*, is defined to be one that is invariant under the RG transformation :

$$S^* = R_b(S^*) = \sum_a K_a^* S_a^* \qquad (8)$$

In the subsequent work we shall assume the existence of at least one fixed point. From (7) and (8) we conclude that the fixed point must lie in a subspace $\xi = \infty$ (or, trivially $\xi = 0$) of the coupling constant space.

If we assume that the renormalized couplings $\{K_a^{(n+1)}\}$ are analytic functions of the unrenormalized ones $\{K_a^{(n)}\}$ then we can linearize the RG transformation (6) in the neighbourhood of a fixed point. This assumption is not unreasonable as the RG transformation involves only one scale and it is expected that the critical singularities arise from the repeated application of the RG and not from the functional dependence of $\{K_a^{(n+1)}\}$ on the $\{K_a^{(n)}\}$. Thus, we write

$$K_a^{(n+1)}(K_b^{(n)}) = K_a^{(n+1)}(K_b^*) + (K_b^{(n)}-K_b^*) \left.\frac{\partial K_a^{(n+1)}}{\partial K_b^{(n)}}\right|_{K^*} + \ldots \quad (9)$$

Neglecting terms $O[(K_b^{(n)} - K_b^*)^2]$ and using the relation $K_a^{(n+1)}(K_b^*) = K_a^*$ we obtain the linearized RG transformation

$$\Delta K_a^{(n)} = T_{ab}\Delta K_b^{(n)} \quad (10)$$

where T_{ab} is a linear realization of the RG transformation near a fixed point. Denote its eigenvectors and eigenvalues by $h^{a'}$ and $\lambda^{a'}$ respectively ($a' = 1, 2, \ldots$) and the corresponding interactions by $h^{a'}(U)$ where $\{U\}$ are the configuration matrices:

$$h^{a'}(U) = \sum_a h_a^{a'} S_a(U) \quad (11)$$

Assuming the n^{th} renormalized action is still near enough the fixed point for the linear approximation to apply, we can expand in terms of the eigenvectors $h^{a'}$:

$$S(U) = S^*(U) + \sum_{a'} c^{a'} h^{a'}(U) \underset{(RG)}{\rightarrow} S^*(U) + \sum_{a'} \lambda^{a'} c^{a'} h^{a'}(U)$$

$$\rightarrow \ldots \underset{(RG)}{(n \text{ steps})} \ldots \rightarrow S^*(U) + \sum_{a'} (\lambda^{a'})^n c^{a'} h^{a'}(U) \qquad (12)$$

where the $\{c^a\}$ are constants. This expansion is of course carried out with the usual reservations coming from the fact that T_{ab} is an infinite matrix.[50]

Eq.(12) shows that those interactions with $\lambda^a < 1$ are suppressed after a sufficient number of applications of the RG transformation. These are called 'irrelevant' and do not contribute to the fixed point action. On the other hand the effect of those interactions with $\lambda^a > 1$ is growing with each application of the RG transformation. They are called 'relevant' interactions. Finally, the operators corresponding to $\lambda^a = 1$ are 'marginal' and their effect can only be determined by higher order calculations. In most practical situations the largest eigenvalue is greater than one but there may be more than one relevant operator associated with a given fixed point.

The picture so far is as follows. Starting on the critical surface, the sequence of renormalized actions remains entirely in that surface, as can be seen from (7). Once in the neighbourhood of an attractive fixed point, the RG transformation will bring the

action to that fixed point. However, starting slightly off the critical surface but still in the neighbourhood of an attractive fixed point the action will initially converge towards that fixed point. Because of the smooth dependence of the renormalized couplings on the unrenormalized ones, the renormalized action will stay close to the critical surface and the fixed point until the effect of the relevant operators in (12) becomes large and the action moves away from the critical surface, along some 'relevant' direction, called the renormalized trajectory (RT). This situation is (very) schematically depicted in Fig.1.

The eigenvalues of the linearized RG matrix T_{ab} determine the rate at which the sequence of transformations converges to the fixed point. They can be related to the critical exponents of the model. For example, consider λ_1 and assume it is the largest eigenvalue (and greater than 1). Then, near the critical temperature T_c, we have

$$(T - T_c)' \sim \lambda_1 (T - T_c) \tag{13}$$

From (7), (13) and $\xi \propto |T-T_c|^{-\nu}$ where ν is a critical exponent, we find

$$\nu = \ln b / \ln \lambda_1 \tag{14}$$

Other exponents can be similarly determined e.g. from the existence of symmetry breaking terms in the Hamiltonian and from the scaling relations.

In practical calculations, because of the infinite number of dimensions in the parameter space, one has to impose approximations which eliminate all but a small number of interactions. This is called truncation. In principle approximations may be improved by including more couplings. In practice, in view of the calculational difficulties associated with a large coupling space, this is usually a very difficult procedure.

In conclusion, it may be said that the usual real-space RG truncation methods, despite their promising outlook involve, at present, uncontrollable approximations which are not systematically improvable.

2B. THE MONTE-CARLO RENORMALIZATION GROUP METHOD

In Sec.1A we reviewed the real space renormalization group formalism and mentioned the calculational difficulties associated with the usual truncation methods. Here we describe a numerical scheme which largely avoids these difficulties.

The Monte-Carlo Renormalization group (MCRG) is a combination of standard Monte Carlo techniques with Real Space Renormalization Group analysis [51]. Obviously, since a finite lattice has to be used, some truncation will be made. But, as will be discussed below, the effects of this approximation are both controllable and systematically improvable. The method is readily applicable to lattice gauge theories (with some care) [52], as well as spin systems [53].

The method can be described as follows. For illustration purposes we use a spin system. (The extra complication arising from local gauge invariance will be addressed to later on.) We start from the unrenormalized Hamiltonian $H^{(0)}$ in an initial configuration of spins. Then, rather than calculate the renormalized couplings directly, we use an MC simulation in the usual manner to generate a number of configurations associated with the given Hamiltonian. The configurations may be stored for future use. Having stored the configurations, we can first of all apply standard MC procedures and measure any expectation value required. Secondly we can apply a local RG transformation to the spins (blocking) without worrying about the effect on the Hamiltonian. This procedure results in a new, 'blocked' configuration corresponding to a (yet unknown) re-

normalized Hamiltonian $H^{(1)}$. Obviously the whole process can be repeated. The renormalized couplings and the RG matrix T_{ab} can then be extracted, as will be seen, from the expectation values computed at each blocking stage.

The procedure outlined above involves two distinct types of approximation (truncation). Firstly, the renormalized Hamiltonian on the finite lattice is used to represent the corresponding infinite lattice Hamiltonian. Naturally only those interactions whose range can fit the lattice size can be included. However, the number of such interactions is much larger than in the usual truncation approximations (order of thousands). All the corresponding renormalized couplings are implicitly accounted for. This of course assumes that the effective range of the renormalized Hamiltonians is smaller than the size of the lattice.

The second type of truncation is made in the actual calculation of the linearized RG matrix T_{ab} (whose eigenvalues yield the critical exponents). It is infinite-dimensional and only a finite part of it can be calculated. However the parameter space can be enlarged by introducing more operators into the simulation. In contrast to analytical methods, this can be done without a major increase in programming effort (or execution time). The effect of these extra operators can be monitored and their approach to the fixed point observed. Thus, this approximation is systematically improvable. In Sec.3 we analyse the U(1) model first with just fundamental-adjoint action and then with a 5-operator action and we find that while the extra operators are irrelevant, convergence is substantially improved.

The algorithm for evaluating the critical exponents is relatively simple as it does not involve a calculation of the renormalized Hamiltonians. We calculate numerically the linearized RG matrix T_{ab} which, from (10) is given by

$$T_{ab} = \left. \frac{\partial K_a^{(n+1)}}{\partial K_b^{(n)}} \right|_{K^*} \tag{15}$$

To compute T_{ab} we first change variables in

$$\frac{\partial \langle S_c^{(n+1)} \rangle}{\partial K_b^{(n)}} = \sum_a \frac{\partial K_a^{(n+1)}}{\partial K_b^{(n)}} \frac{\partial \langle S_c^{(n+1)} \rangle}{\partial K_a^{(n+1)}} \tag{16}$$

The derivatives in either side are obtained from connected correlation functions, namely

$$\frac{\partial \langle S_a^{(n)} \rangle}{\partial K_b^{(m)}} = \langle S_a^{(n)} S_b^{(m)} \rangle - \langle S_a^{(n)} \rangle \langle S_b^{(m)} \rangle \tag{17}$$

which are computed in the MC simulation. (Note that the left-hand side of (16) may involve computation of correlations between different blocking levels.)

In some cases the accuracy can be improved by choosing operators whose expectation values vanish on a finite lattice due to symmetry, as the second term in the RHS of (17) vanishes. An example is $\sin\theta$ in the U(1) model.

The success of this method depends critically on the ability to start as close as possible to the critical surface. In that case the sequence of renormalized configurations will converge towards the fixed point. Thus, the method is best suited for application to models whose critical points are known, at least approximately. The consistency of the results for the critical exponents can be tested by regarding two successive RG transformations each with scale factor b, as a single one with scale factor b^2. This would correspond to a transformation matrix T^2. As multiplication of the T matrices is performed implicitly by the MCRG method, effectively taking all interactions that will fit the lattice into account, any discrepancies between exponents for T and T^2 implies that relevant couplings have been neglected.

The methods described so far, as already pointed out, do not require the determination of the renormalized parameters. However, in order to realise the full potential of the MCRG methods one must be able to locate the fixed point and determine the flows of the coupling constants in its neighbourhood. Early attempts used a 'two-lattice comparison' in which one compared expectation values obtained from independent MC simulations on two lattices of the same size and boundary conditions (thus eliminating finite size effects). Each of the two lattices was the result of blocking transformations and originated from starting lattices of different sizes. Ref.[54] is an example of the application of this method to the 3-d Ising model. Although in principle coupling constant trajectories can be

determined with this method, in practice the errors associated with finding the differences between results of two simulations limit its applicability.

We now describe a more recent method, due to Swendsen [55]. The method is more general in that it is equally applicable to lattice gauge theories and spin systems and does not rely on the simulation being performed near the critical surface. The basic idea is to construct two independent expressions for the expectation value of a given operator. One of them is the usual expression for the expectation value and does not depend explicitly on the couplings. The other depends implicitly as well as explicitly on a set of properly chosen 'trial' couplings. By minimising the differences between the two, we assert that the trial parameters will converge towards the actual ones. Moreover, the method lends itself to iterative application eventually converging to the actual couplings.

We illustrate the method for a U(1) gauge theory with a multi-coupling action as given in (1):

$$S = \sum_{a} K_a S_a \qquad (18)$$

where, as usual factors of the inverse temperature etc. are included in the definition of the coupling constants. For U(1):

$$S = \beta_F \sum_{p} \cos\theta_p + \beta_A \sum_{p} \cos 2\theta_p + \ldots \qquad (19)$$

where β_F and β_A are the fundamental and 'adjoint' couplings and p stands for plaquette. Then the expectation value of S_B is given by

$$\langle S_B \rangle = Z^{-1} \operatorname*{Tr}_{\{\theta_\ell\}} S_B \, e^{-S} \tag{20}$$

where

$$Z = \operatorname*{Tr}_{\{\theta_\ell\}} e^{-S} \tag{21}$$

and we have denoted the integration measure by

$$\operatorname*{Tr}_{\{\theta_\ell\}} = \int_0^{2\pi} \prod_\ell \frac{d\theta_\ell}{2\pi}$$

We now want an alternative expression for $\langle S_B \rangle$, one which depends explicitly on a set of known, 'trial' couplings. To this end, consider a single link ℓ in the lattice and define

$$S_{F,\ell} = \sum_{p' : \ell \in p'} \cos\theta_{p'} \tag{22}$$

where the sum is taken over those plaquettes p' that contain the link ℓ. Clearly the sum has $m_F = 6$ terms in 4-dimensions. Then

$$S_F = \frac{1}{m_A} \sum_\ell S_{F,\ell} \tag{23}$$

and the same construction can be generalised to other operators

$$S_a = \frac{1}{m_a} \sum S_{a,\ell} \tag{24}$$

Define the action s_ℓ over a single link ℓ as

$$s_\ell = \sum_a K_a S_{a,\ell} \tag{25}$$

and the partition function

$$z_\ell = \operatorname*{Tr}_{\{\theta_\ell\}} \exp(-s_\ell) \tag{26}$$

So we can define an expectation value for $S_{a,\ell}$ in a fixed background:

$$\langle S_{a,\ell} \rangle_\ell = z_\ell^{-1} \operatorname*{Tr}_{\{\theta_\ell\}} S_{a,\ell} \exp(-s_\ell) \tag{27}$$

Note that the eq.(27) is a function of those link variables that are connected through the action to θ_ℓ. With these definitions we can construct a new expression for the expectation value $\langle S_a \rangle$:

$$\langle S_a \rangle = \frac{1}{m_a} \sum_\ell \langle S_{a,\ell} \rangle \tag{28}$$

where

$$\langle S_{a,\ell}\rangle = Z^{-1} \operatorname*{Tr}_{\{\theta_i : i\neq\ell\}} \exp[-(S-s_\ell)] z_\ell \langle S_{a,\ell}\rangle_\ell \qquad (29)$$

Now equation (29) can easily be evaluated in an MC simulation (it can even be evaluated analytically in some cases) because it involves tracing over a single variable. Moreover, we can introduce an independent, 'trial' set of couplings $\{K_a\}$ in (27) and perform the simulation with respect to the trial couplings. Then (29) is evaluated (and hence (28)) by summing over configurations. This results in a 'trial expectation value'

$$\begin{aligned}\langle \tilde{S}_a\rangle &= \frac{1}{m_a} \sum \langle \tilde{S}_{a,\ell}\rangle \\ &= \frac{1}{m_a} \sum_\ell \langle \langle \tilde{S}_{a,\ell}\rangle_\ell\rangle \end{aligned} \qquad (30)$$

where, as in (29) the outer brackets denote expectation values with respect to the original couplings. According to ref.[55],

$$\langle \tilde{S}_a\rangle = \langle S_a\rangle \qquad \text{if and only if } \{\tilde{K}_b\} = \{K_b\} \qquad (31)$$

for all a and b. Thus, to first order in

$$\delta\tilde{K}_b = \tilde{K}_b - K_b \qquad (32)$$

we have

$$\tilde{\langle S_a \rangle} - \langle S_a \rangle = \sum_b \frac{\partial \tilde{\langle S_a \rangle}}{\partial \tilde{K}_b} \delta \tilde{K}_b \qquad (33)$$

and the derivatives in (33) are as always computed from connected correlation functions:

$$\frac{\partial \tilde{\langle S_a \rangle}}{\partial \tilde{K}_b} = \frac{1}{m_a} \sum_{\ell} \langle\langle \tilde{S}_{a,\ell} \tilde{S}_{b,\ell} \rangle_\ell - \tilde{\langle S_{a,\ell} \rangle}_\ell \tilde{\langle S_{b,\ell} \rangle}_\ell \rangle \qquad (34)$$

The relations (32), (33) and (34) can then be used to reconstruct the renormalized parameters in the Hamiltonian. A check of the consistency of this method is to reproduce the known couplings of the starting action. Of course, the trial couplings must be close to the actual couplings otherwise eq.(33) does not apply. Thus in most cases a preliminary calculation has to be made to determine a good set of trial couplings. This was done relatively easily in most cases.

3. COMPUTATIONAL ASPECTS

A. GENERAL

The computations involved in this work were carried out at the Distributive Array Processor (DAP) at Queen Mary College. The DAP is a parallel processing machine, capable of performing simultaneous operations on the contents of its store, provided these are mapped into 64 x 64 arrays of processing elements. Such machines are ideal for Monte-Carlo work because they allow for compact and efficient algorithms in which the link variables are mapped into batches of 4096 and updated concurrently. In our U(1) application we found the updating speed to be 160000 links per second.

Throughout the numerical simulations we used the group Z(64) as an approximation to U(1). In this approximation the gauge group elements are realised by the 64 angles which are integer multiples of $\pi/32$ in the range $(0, 63\pi/32)$. Thus, each angle is uniquely associated with an integer variable and intermediate arithmetic can be performed in integer*1 mode while it is possible to store the values of four link variables in a single address. This resulted in substantial savings both in simulation time and in storage memory requirements. A 'look-up' table was provided which converted any required integer*1 variable into the corresponding cosine at the end of the calculation.

Some care must be exercised during the updating procedure. In order to ensure convergence to equilibrium one should not update simultaneously variables that interact with one another through the

action. We have taken advantage of the logical facilities provided by DAP Fortran to separate each 64x64 bit-plane into 'even' and 'odd' sites alternating in every direction. By processing the even and odd variables independently one ensures that each link is updated in a constant background.

For each value of the couplings used we have started from a random configuration which was brought to equilibrium after 60000 Monte-Carlo updates. We have used the standard Metropolis algorithm [35] with one hit per link which was found to give a satisfactory acceptance rate of about 30% in the viscinity of the phase transition.

Our data come entirely from simulations on 8^4 lattices. Where appropriate we have included data from 16^4 simulations as reported in ref.[56]. Upon blocking down from and 8^4 lattice, we have exploited the parallel nature of the DAP to keep and processed simultaneously all the resulting 4^4 lattices (16 of these) and 2^4 lattices (256 of these). This improved the statistics considerably. The CPU time required for a complete Monte-Carlo cycle was approximately 2.25 seconds for the critical exponents calculation and 8 seconds for the renormalized coupling calculation.

In the neighbourhood of the phase transition we have observed the two-state and metastability effects reported in [28]. Near the phase transition we have therefore performed very long simulations to ensure that the average lifetime of each metastable state was much less than the total simulation time.

B. THE BLOCKING PROCEDURE

For lattice gauge theory, an important restriction in performing the blocking transformation is that it must preserve the gauge invariance of the theory. Early attempts overcame this problem by introducing gauge-fixing [57]. However this is undesirable for Monte-Carlo simulations since it introduces long relaxation times and is time-consuming when employed in the definition of the renormalized operators. The first successful attempt which avoids gauge-fixing is described in ref.[52]. A version of that method which is suitable for U(1) lattice gauge theory is as follows (Fig.2):

The renormalized link A'B' is assigned an angle $\theta_{A'B'}$ which contains contributions from products of gauge group elements along paths leading from A' to B'. We have considered the following paths (refer to Fig.3)

P_0 : AFB (straight line path)
P_1 : ACDEB
P_2 : ACDFB
P_3 : AFDEB

Of course, for each path other than the straight line one, we sum over all directions and orientations.

An important consideration here is that the position of the fixed point is not universal but depends on the details of the blocking procedure. Since on a 8^4 lattice there are only two blocking steps available, it is important to adjust the blocking procedure so as to move the fixed point as near as possible to the starting point of the original simulation. Therefore the paths are

weighed with external parameters ρ_0, ρ_1, ρ_2 and ρ_3 respectively. This allows the possibility of optimising the blocking transformation. Of course we must have $\rho_2 = \rho_3$ from symmetry.

For programming purposes, an efficient way (for U(1)) of calculating the renormalised link $\theta_{A\,B}$ is:

$$\tan\theta_{A'B'} = \frac{\rho_0\sin\theta(P_0) + \rho_1\Sigma\sin\theta(P_1) + \rho_2\Sigma\sin\theta(P_2) + \rho_3\Sigma\sin\theta(P_3)}{\rho_0\cos\theta(P_0) + \rho_1\Sigma\cos\theta(P_1) + \rho_2\Sigma\cos\theta(P_2) + \rho_3\Sigma\cos\theta(P_3)} \qquad (18)$$

where $\theta(P)$ denotes the sum of oriented link angles along the path P and the sums in eq.(18) are over all (six) orientations of the non-straight line paths. It can be easily shown that eq.(18) preserves local gauge invariance for gauge transformations on those lattice sites which are retained in the new lattice.

4. RESULTS AND DISCUSSION

A. THE CRITICAL EXPONENTS

In this subsection we report on measurements of the critical exponents of U(1) lattice gauge theory, using the method outlined in Sec.2B, eqs.(14)-(17). We have used an action containing 5 operators, namely the fundamental and adjoint plaquette, the six-link flat, six-link bent and six-link 'arm-chair' operators. We have also examined the effect on the measurements of varying the blocking procedure.

The algorithm for the calculation of the critical exponents relies on the ability to simulate very near the critical surface. We have used the β values 1.0060, 1.0065, 1.0070, 1.0075 and 1.0080 at each of which we have carried out 6400 Monte-Carlo iterations each separated from the previous one by 10 further updates to minimize correlations between measurements. The errors on the measurements were estimated on the basis of a statistical analysis on the expectation values [39].

It was observed that up to the value of $\beta = 1.0065$ the measured expectation values decreased very rapidly at successive blocking levels. This suggests that the system is far from criticality already after the blocking step.

In Table 1 we show the largest eigenvalue at each blocking step, both for the fundamental-adjoint and the full 5-operator actions. These results appear to be quite stable with relatively small statistical fluctuations, especially for the β values further

away from criticality. In the viscinity of the critical region the main contribution to the largest eigenvalue comes from the fundamental and adjoint operators suggesting that the effect of the other operators is negligible. Further evidence for this comes from measuring the eigenvalue for blocking from an 8^4 down to a 2^4 lattice in one step. These results are also shown in Table 2. In all cases, that eigenvalue is very nearly the product of the two eigenvalues resulting from blocking from 8^4 to 4^4 and from 4^4 to 2^4 size lattices. As pointed out in Sec.IIB, this is a signal that no important couplings have been neglected.

The results for the measurement of the critical exponent are shown in Table 2 and plotted in Fig.3. These are calculated from the largest eigenvalue from eq.(14). On the first blocking step step ($8^4 \rightarrow 4^4$) the measured value of the exponent is roughly 0.52, in agreement with refs.[31] and [58] and with the expected behaviour in the neighbourhood of a tricritical point, as mentioned in Sec.I2. However, on the second blocking step ($4^4 \rightarrow 2^4$) the exponent seems to fall to a value of around 0.40 which would be associated with the approach towards an ordinary critical point. We also observed a slight systematic increase of the value of the exponent as β is increased towards the critical point. This is also in agreement with ref.[58].

Despite the fact that on blocking from an 8^4 to a 4^4 lattice we measure a tricritical exponent, we do not see a second relevant eigenvalue (ie greater than 1) as would be expected in the neighbourhood of a tricritical point. The results for the second largest eigenvalues are tabulated in Table 3 and they have also

been well determined with relatively small statistical fluctuations. This implies that after the first blocking step the system is already far from the linear region of the tricritical point although the starting point of the simulation (at the Wilson axis) might still have been close to it.

So the overall picture is that the renormalization group transformation moves the system away from a linear region of a tricritical point and into a linear region associated with an ordinary fixed point. This is in agreement with similar measurements reported in ref.[56] on 16^4 lattices where the exponent show a clear change from a value of around 0.5 at the first blocking step to one of around 0.34 at the third blocking step. However, it is not known whether the system really is near a fixed point associated with an ordinary critical point, even after the last blocking step. Although the measured value of around 0.35 agrees with earlier determinations of the critical exponent, as reported in Sec.I2, on our measurements this could only be a transient effect, as the system moves towards the fixed point. To answer this question conclusively we would have to be able to simulate on much larger lattices, so as to have more blocking steps available. However, evidence that this is indeed the case comes from changing the blocking procedure, as pointed out in Sec.3B.

The results shown so far, in Tables 1-3 and fig.3 all refer to a simple blocking procedure in which the parameters ρ_0, ρ_1, ρ_2 and ρ_3 as defined in Sec.3B were set to the values 1, 1, 0 and 0 respectively. We have repeated the calculation at the β values of 1.0065 and 1.0075 but this time using a blocking procedure in which

the contribution from the central link was increased to $\rho_0 = 10$ with the other parameters retaining the same values. The results are shown in Table 4 in the left-hand column. We have included for comparison the corresponding results from the earlier simulation.

These results now show clear evidence of a fixed point behaviour particularly at $\beta = 1.0075$ where the measured value of the exponents at the two blocking steps are within the statistical uncertainties of each other at 0.351 ± 0.011 and 0.338 ± 0.014. Such a result confirms the conjecture presented in ref.[58] where the measured values of the exponent were extrapolated to β_c^{∞} at which point the changes between different blocking levels seemed to vanish, and is also in very good agreement to other measurements using conventional Monte-Carlo techniques as summarized in Section I2.

4B. THE RENORMALIZED PARAMETERS

We have applied the Swendsen method [55], as outlined in Sec.2B to reconstruct the flows of the coupling constants under the Renormalization Group blocking transformation. We have used an 8^4 lattice and simulated with an action containing five operators as described at the beginning of Sec.4A.

Some consideration was given to the problem of finding the best way to evaluate the trial expectation values, eqs.(27)-(29) or (30). This is important because this part of the calculation requires a great deal of computing time. The integrals in eq.(27) are over a single link variable and would have been exactly solvable but for the presence of the adjoint term in cos 2θ in the action eq.(25). After considering various alternative approximate methods we decided that the most efficient way to evaluate eq.(27) was by another Monte-Carlo simulation. Thus, within each configuration in the original simulation, we perform a number N_H of Metropolis updates on the link ℓ, keeping its background fixed as required by eq.(27). The results for the required correlations, eqs.(30) and (34), are then accumulated over the total number N_S of configurations in the main simulation.

Some preliminary runs were made to determine a good value for N_H. The answer depended on the values of the trial couplings used. We found that provided all trial couplings except the fundamental were set to zero, then decreasing the value of N_H down to about 5

did not make a significant difference to the computed trial expectation values. In such cases therefore we have used a value of $N_H = 8$.

However, if the computation of the trial expectation values involved other non-zero couplings, then we found that a much higher value of N_H was required before the trial measurements reached thermal equilibrium. This was the case in the spin-wave phase of the model. In that case we used a value of $N_H = 40$. This resulted in considerably longer computing time requirements.

We have used the starting values (on the Wilson axis) of β = 1.0070, 1.0080 and 1.0130. Of these, the first two are in the strong coupling phase of U(1) and the third is in the spin-wave phase. The starting configurations (except at $\beta = 1.013$) were the corresponding final configurations from the critical exponents configuration and further equilibriated by 60000 sweeps through the lattice. We have not performed a fixed number of Monte-Carlo iterations but for each run monitored the evolution of both actual and trial expectation and averaged over a suitable range in the simulation. We did, however, observe the metastability effects reported in ref.[31] and consequently found it necessary to perform very long simulations, exceeding 18000 sweeps. Furthermore, it was observed that if the averaging was performed only within one of the metastable states, the results for the coupling flows appeared to qualitatively follow the pattern of the particular side of the phase transition they corresponded to.

The results for various starting β values on the Wilson axis are shown in Tables 5(a)-(e) where we have also examined the effect of varying the blocking procedure (Tables 5(c) and (d)). The same results are reproduced in Fig.4, where two distinct Renormalization Group behaviours on either side of the phase transition can be clearly seen.

On the strong coupling phase (small β) the Renormalization Group drives the system towards the trivial fixed point at the origin, as expected. The results for the blocking procedure corresponding to $\rho_0 = \rho_1 = 1$ and $\rho_2 = 0$ (represented by dashed lines in Fig.5) are in good agreement with the two-operator calculations of ref.[56]. Changing the blocking parameters while remaining on the strong coupling phase does not change the pattern of the Renormalization Group flows qualitatively. The solid lines in Fig.4 correspond to a blocking with $\rho_0 = 8$, $\rho_1 = 1$ and $\rho_2 = 0$ where the approach to the trivial fixed point is even faster and the adjoint coupling becomes slightly negative after the first blocking step. In all cases, as can be seen from Tables 5(a)-(d) the contribution of all the other couplings except the fundamental to the renormalized Hamiltonian remains negligible and the system is driven quite far away from the critical boundary even after one blocking step. This lends evidence to the conclusion, already stated in refs.[56] and [58] and in the previous subsection that there are no further relevant operators in the U(1) action.

On the spin-wave phase (large β) the behaviour is quite different, as can be seen from Table 5(e). As pointed out at the beginning of this subsection, the runs on this side of the phase

transition were slower by a factor as high as 80% because of the non-trivial values of the trial couplings required. This had a serious effect on our statistics and also prevented us from examining the effects of varying the blocking procedure. Our results, obtained from a blocking with $\rho_0 = \rho_1 = 1$ and $\rho_2 = 0$ are shown in Table 5(e)and also in Fig.4. It is evident that there is a dramatic qualitative change in the Renormalization Group behaviour on this side of the phase transition. However our results do not show the expected convergence towards the fixed line [19], although such a conjecture would not be entirely out of place, given the fact that the results on the final blocking step (2^4 lattice) probably suffer from large systematic finite size effects, as pointed out in ref.[56]. As can be seen from Table 5(e), the effect of the more non-local operators to the renormalized action is now considerably greater. We do not know however whether this is a genuine effect due to the existence of more relevant operators or simply because the starting action on the Wilson axis was too far away from the fixed point. This question could be resolved either by simulating on larger lattices so as to have more blocking steps available (and possibly with higher statistics) or (more cheaply) by using an 8^4 lattice and finding an optimal blocking procedure which would bring the fixed point as near as possible to the starting point of the simulation. Although either approach would be computationally rather demanding, the matter is interesting and clearly merits further attention.

5. CONCLUSIONS

In this Chapter we have applied the powerful methods of MCRG to the U(1) lattice gauge model. We have been able to measure a critical exponent which is in good agreement with all similar previous determinations [17-20, 56, 58, 59] and elucidate the different Renormalization Group behaviours of the theory on either side of the phase transition. Undoubtedly the MCRG is a strong weapon for handling such problems with obvious possibilities of application in the case of Non-Abelian Gauge Theories.

However, the question of the tricritical point [31] remains an open one. In all the calculations we have used a starting action on the Wilson axis but we did not see a second relevant operator as would be expected in the viscinity of a tricritical point. This means that already after the first blocking step the system is far away from the neighbourhood of a tricritical point although at the starting point it might still have been close to one. Furthermore, the results for the critical exponents suggest that the starting point on the Wilson axis is between the tricritical point and the fixed point associated with a second order phase transition. This implies that the tricritical point is probably above the Wilson axis, in disagreement with ref.[31], although its exact location has not been determined. We expect that simulating further up the phase boundary in the fundamental-adjoint plane (Fig.11), a second relevant eigenvector would emerge, signalling the proximity of a tricritical point. The location of such a point could then be determined by the MCRG

method, as well as its precise nature and the associated tricritical and subsidiary exponents. Such a calculation would be rather difficult, however, because of the presence of an adjoint component in the simulation and because of the usual problems associated with simulating in the neighbourhood of a tricritical point where both long relaxation times and metastability effects would have to be dealt with. Moreover, the calculation could be repeated in momentum space (Sec.1A) which would allow for smaller scale changes in the Renormalization Group transformation and perhaps therefore give an indication of the size of the linear and cross-over regions around the tricritical point.

In summary, we can state that the potential of the MCRG method has been amply demonstrated. All our results are consistent with the presence of a second order phase transition in U(1) lattice gauge theory on the Wilson axis, as also pointed out in Chap.II on the basis of a conventional Monte-Carlo analysis on the simplicial lattice. The behaviour of the system under the Renormalization Group is what would be expected from (a) a Gaussian (trivial) theory on the strong coupling phase and (b) a theory with algebraic correlations in the spin-wave phase.

TABLE 1

β	Number of Operators	Largest eigenvalue		
		$8^4 \to 4^4$	$4^4 \to 2^4$	$8^4 \to 2^4$
1.006	5	3.93(7)	6.50(9)	26.36(12)
	2	3.63(2)	5.72(6)	21.08(9)
1.0065	5	3.85(5)	6.32(11)	24.91(14)
	2	3.63(2)	5.72(8)	19.70(11)
1.007	5	3.80(6)	6.21(11)	22.47(12)
	2	3.61(3)	5.69(10)	19.56(9)
1.0075	5	3.75(8)	5.85(19)	21.13(19)
	2	3.60(1)	5.61(11)	19.48(10)
1.008	5	3.70(5)	5.47(10)	19.34(18)
	2	3.59(3)	5.54(10)	19.85(15)

Table 1 The largest eigenvalue of the RG matrix measured at various values of β and blocking levels. The two operators are the fundamental and adjoint plaquette. The five operators are the two plaquette operators and the three six-link operators. The numbers in brackets indicate the statistical uncertainty in the least significant digits.

TABLE 2

β	Exponent ν	
	$8^4 \to 4^4$	$4^4 \to 2^4$
1.0060	0.51(2)	0.37(2)
1.0065	0.51(1)	0.38(1)
1.0070	0.52(1)	0.38(1)
1.0075	0.52(1)	0.39(1)
1.0080	0.53(1)	0.41(1)

Table 2 The exponent ν measured from an 8^4 simulation with 5 operators.

TABLE 3

β	Second eigenvalue		
	$8^4 \to 4^4$	$4^4 \to 2^4$	$8^4 \to 2^4$
1.006	0.50(5)	0.75(6)	0.75(6)
1.0065	0.51(5)	0.76(5)	0.76(8)
1.007	0.52(6)	0.81(4)	0.75(8)
1.008	0.51(5)	0.91(5)	0.70(7)

Table 3 The second largest eigenvalue of the RG matrix measured in an 8^4 simulation with 5 operators.

TABLE 4

β = 1.0065

	Exponent ν	
	(a)	(b)
$8^4 \rightarrow 4^4$	0.51(1)	0.34(2)
$4^4 \rightarrow 2^4$	0.38(1)	0.34(2)
$8^4 \rightarrow 2^4$	0.45(1)	0.32(1)

β = 1.0075

	Exponent ν	
	(a)	(b)
$8^4 \rightarrow 4^4$	0.52(1)	0.36(2)
$4^4 \rightarrow 2^4$	0.39(1)	0.33(2)
$8^4 \rightarrow 2^4$	0.45(1)	0.35(2)

Table 4 The critical exponent ν measured at β = 1.0065 and β = 1.0075 using two different blocking schemes. Columns (a) refer to blocking with the parameters ρ_0, ρ_1, ρ_2 and ρ_3 (defined in Sec.3B) set to the values 1, 1, 0 and 0 respectively. In columns (b) the blocking scheme was with ρ_0 = 10, ρ_1 = 1, ρ_2 = ρ_3 = 0.

TABLE 5 (cont'd)

(d)

Operator	Lattice size 8^4	4^4	2^4
1	1.0080	0.539(18)	0.012(19)
2	0	-0.026(16)	-0.001(16)
3	0	-0.019(13)	-0.001(15)
4	0	0.000(15)	0.002(13)
5	0	0.042(19)	0.002(17)

$\rho_0 = 8 \quad \rho_1 = 1 \quad \rho_2 = 0$

(e)

Operator	Lattice size 8^4	4^4	2^4
1	1.0130	0.989(20)	0.931(33)
2	0	0.142(18)	0.260(37)
3	0	0.046(12)	0.038(28)
4	0	0.031(14)	0.020(24)
5	0	0.092(14)	0.093(37)

$\rho_0 = 1 \quad \rho_1 = 1 \quad \rho_2 = 0$

Table 5 The measured values of the renormalized coupling constants at each blocking step for various starting values of β on the Wilson axis and various blocking schemes. The five operators are consecutively the fundamental and adjoint and the three six-link operators.

TABLE 5

(a)

Operator	Lattice size 8^4	4^4	2^4
1	1.0070	0.742(15)	0.311(13)
2	0	0.061(12)	0.029(14)
3	0	0.039(9)	0.012(10)
4	0	0.028(9)	0.006(11)
5	0	0.042(13)	0.019(15)

$\rho_0 = 1 \quad \rho_1 = 1 \quad \rho_2 = 0$

(b)

Operator	Lattice size 8^4	4^4	2^4
1	1.0080	0.761(14)	0.323(15)
2	0	0.069(13)	0.022(14)
3	0	0.039(10)	0.013(12)
4	0	0.030(11)	0.004(12)
	0	0.041(14)	0.025(15)

$\rho_0 = 1 \quad \rho_1 = 1 \quad \rho_2 = 0$

(c)

Operator	Lattice size 8^4	4^4	2^4
1	1.0070	0.517(22)	0.012(19)
2	0	-0.032(14)	0.000(20)
3	0	-0.013(10)	0.000(29)
4	0	0.011(11)	0.000(20)
5	0	0.031(17)	0.001(21)

$\rho_0 = 8 \quad \rho_1 = 1 \quad \rho_2 = 0$

FIGURE CAPTIONS

Fig.1 Schematic representation of the Renormalization Group trajectories where K_1 is assumed to be the only relevant coupling in the problem and all other couplings are shown in the horizontal axis. Trajectories 1 and 2 start slightly away from the critical hypersurface and converge towards the renormalized trajectory. Trajectory 3 starts on the critical hypersurface and converges to the fixed point.

Fig.2 Construction of the renormalized link A'B' from various 'blocking paths' on the original lattice.

Fig.3 The critical exponent ν for various values of β, obtained with a blocking procedure corresponding to $\rho_0 = \rho_1 = 1$ and $\rho_2 = 0$ (see Sec.3B). The crosses represent blocking from an 8^4 to a 4^4 lattice and the dots refer to blocking from a 4^4 to a 2^4 lattice. The error bars represent statistical errors only.

Fig.4 The projection of the RG trajectories of the coupling constants in the β_F-β_A plane. The various starting β-values are represented by crosses (β = 1.0070), dots (β = 1.0080) and open circles (β = 1.0130). Two different blocking schemes are shown, solid ($\rho_0 = 0_1 = 1$, $\rho_2 = 0$) and dotted ($\rho_0 = 8$, $\rho_1 = 1$, $\rho_2 = 0$). Only statistical errors are given.

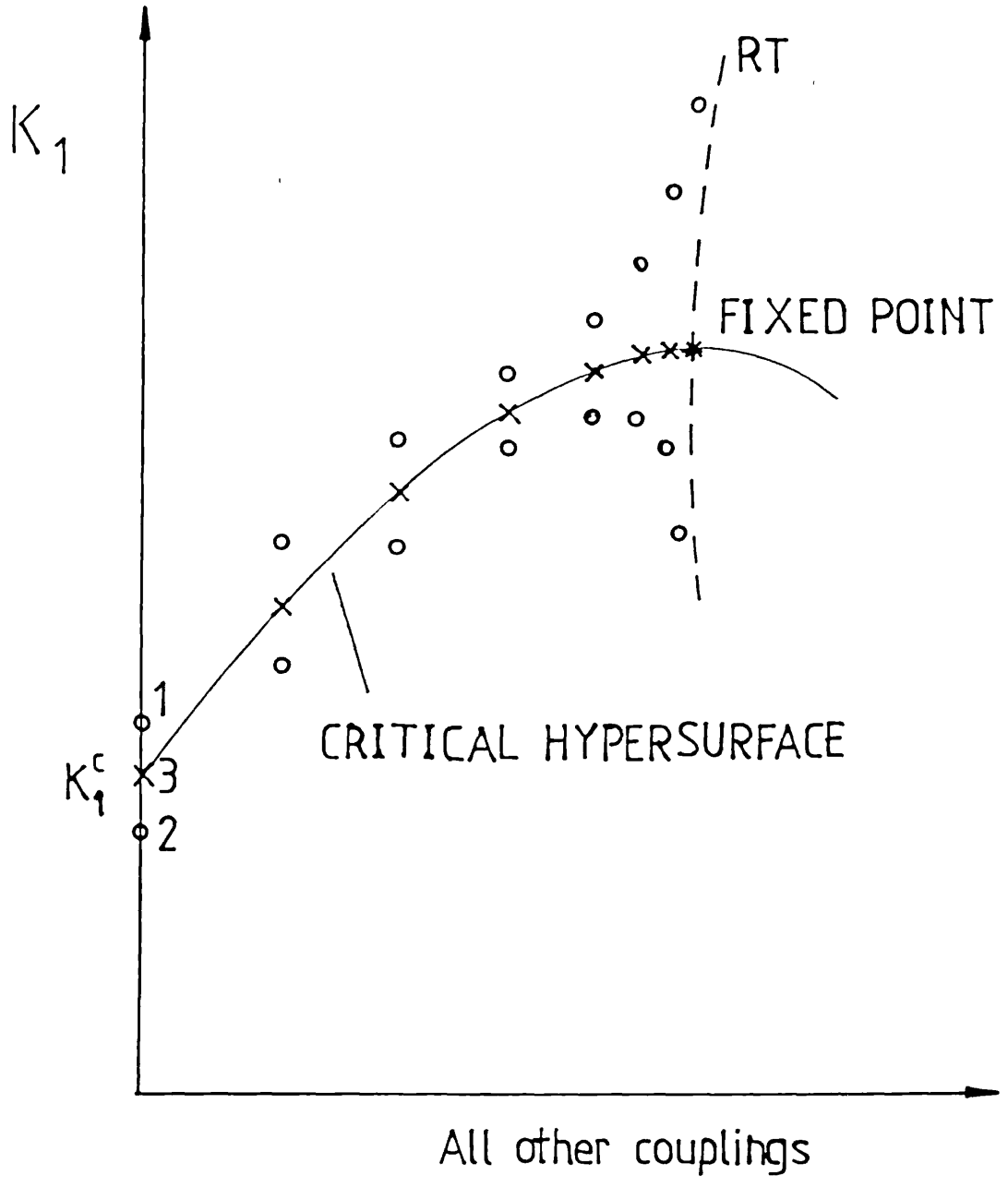
K_1
RT
FIXED POINT
CRITICAL HYPERSURFACE
K_1^c
1
2
3
All other couplings

Fig. 1

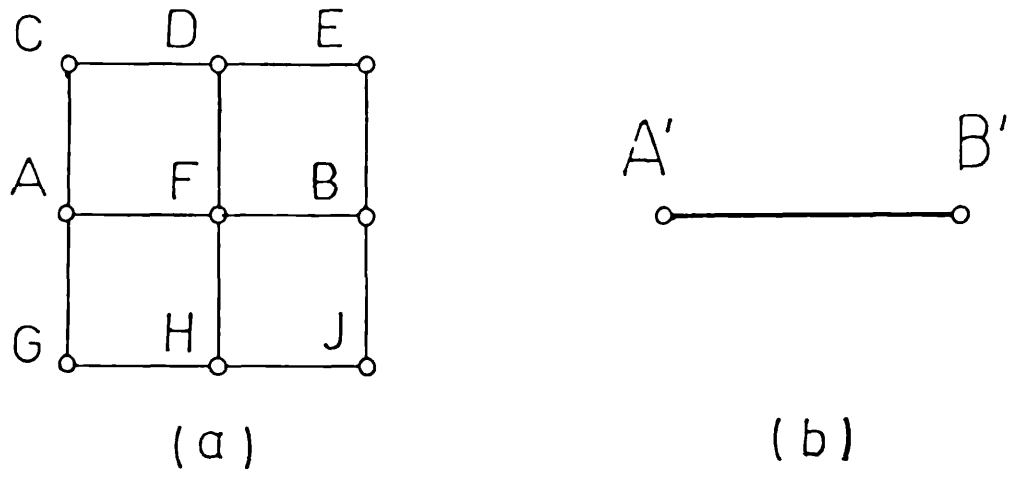

Fig. 2

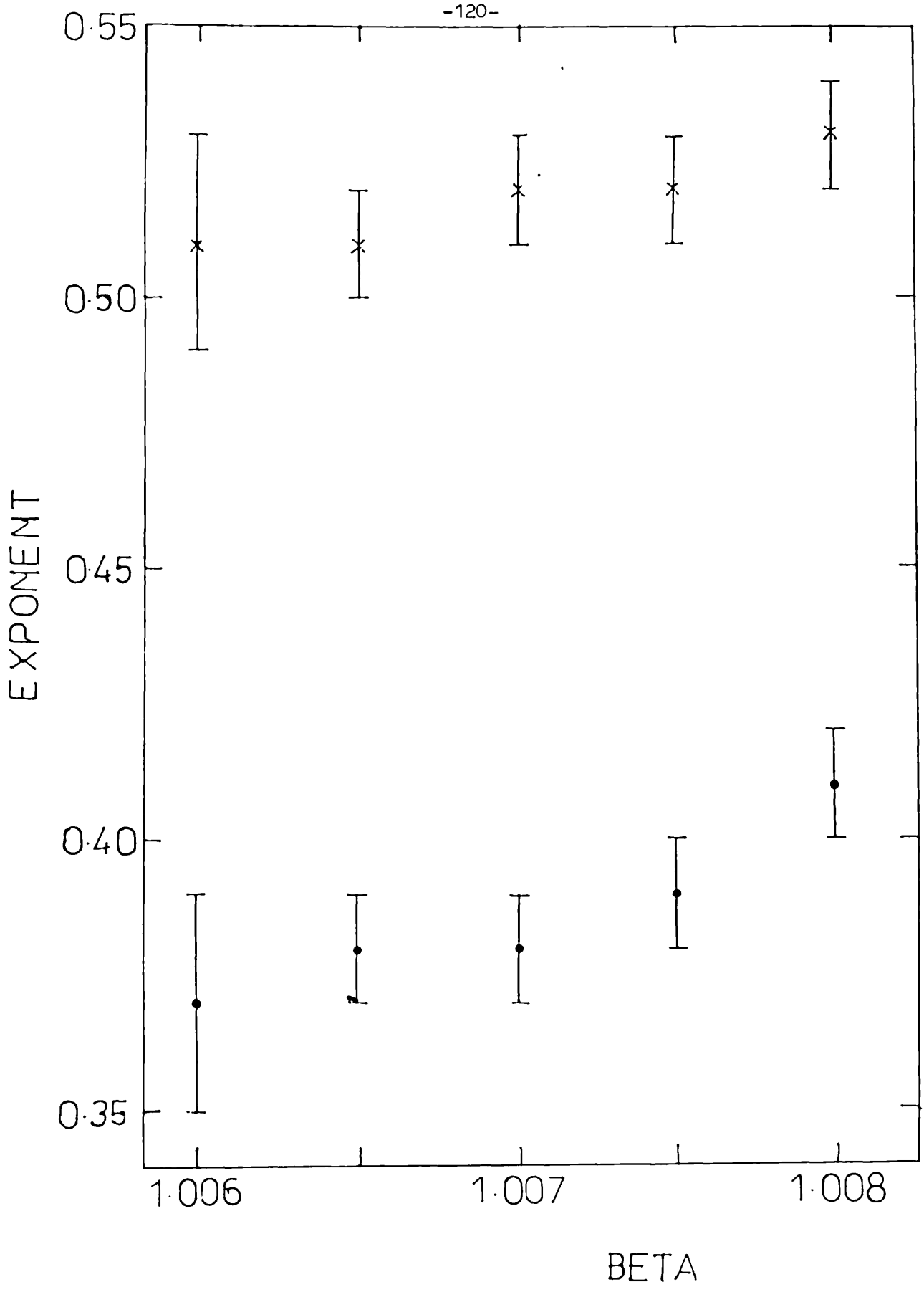

Fig. 3

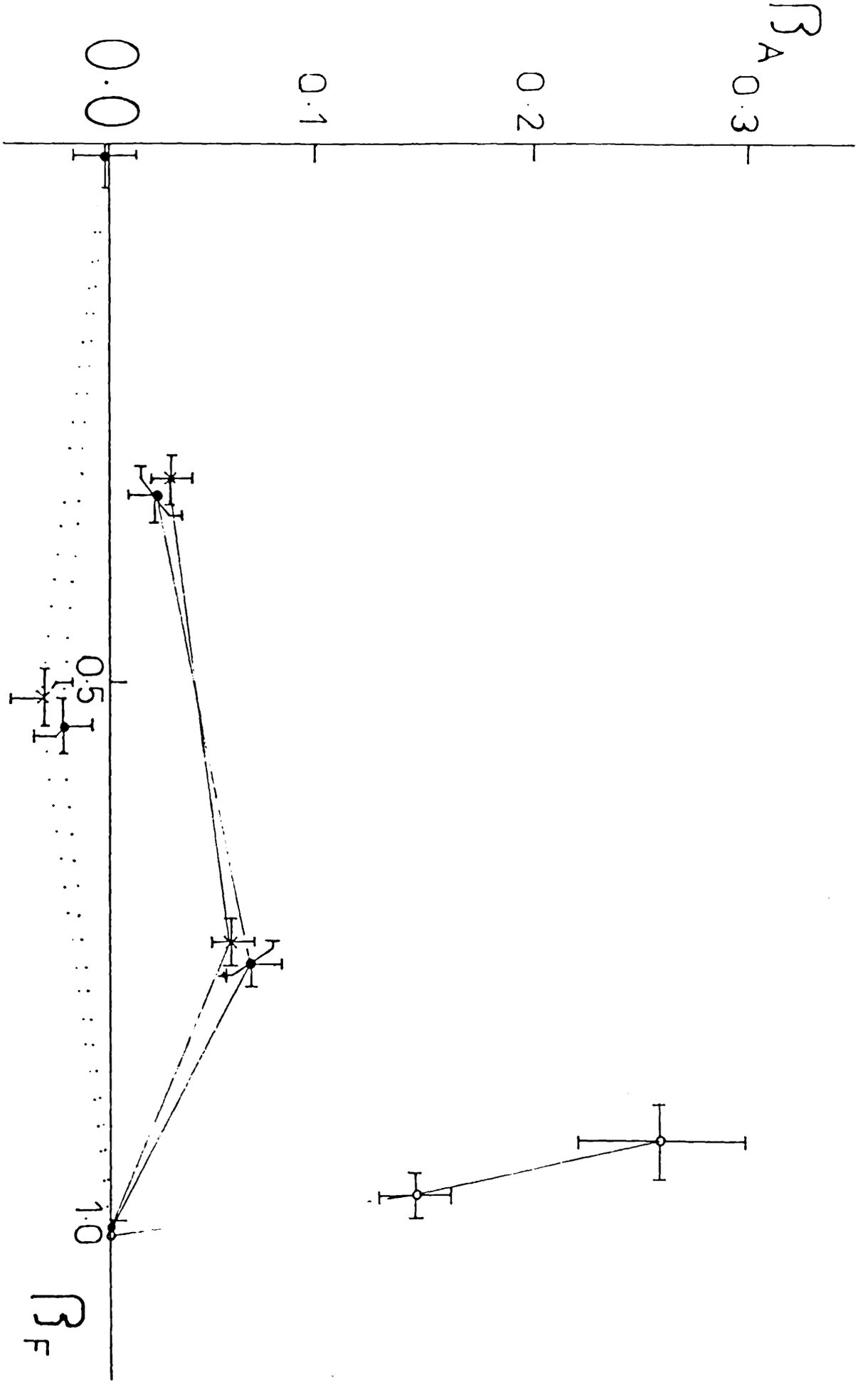
R_A
0.0
0.1
0.2
0.3
0.5
1.0
R_F

REFERENCES

[1] M. Gell-Mann and Y. Ne'eman in "The Eightfold Way", Bengamin, New York (1964)

[2] Y. Nambu; Phys. Rev. Lett. 4, (1960), 380
M. Han and Y. Nambu; Phys. Rev 139B, (1965), 1006
Y. Nambu in "Preludes in theoretical physics" (ed. de De Shalit), North Holland, Amsterdam (1966)

[3] R. Dashen; Phys. Rev 183, (1969), 1291
V. de Alfaro, S. Fubini, G. Furlan and C. Rossetti in "Currents in hadron physics", North Holland, Amsterdam (1973)

[4] F.E. Close in "An introduction to quarks and partons", Academic Press, London (1979)
I.J.R. Aitchinson and A.J.G. Hey in "Gauge theories in particle physics", Hilger, Bristol (1982)
For a review on light-cone singularities and Bjorken scaling, see:
D. Gross in "Methods in field theory"; Proc. of 1975 Les Houches summer school (eds R. Balian and J. Zinn-Justin), North Holland, Amsterdam (1976) and
J. Ellis in "Weak and electromagnetic interactions at high energy", Proc. of 1976 Les Houches summer school (eds R. Balian and C.H. Llewellyn Smith), North Holland, Amsterdam (1977)

[5] D. Gross and F. Wilczek; Phys. Rev. Lett. 30, (1973), 1343 and Phys. Rev. D8, (1973), 3633
H.D. Politzer; Phys. Rev. Lett. 30, (1973) 1346 and Phys. Rep. 14C, (1974), 129

[6] F. Wegner; J. Math. Phys. 12, (1971), 2259

[7] K.G. Wilson; Phys. Rev. D14, (1974) 2455

[8] Lattice reviews include:
J. Kogut; Rev. Mod. Phys. 51, (1979), 659 and Rev. Mod. Phys. 55, (1983), 775

[9] H.B. Nielsen and N. Ninomiya; Nuc. Phys. B185, (1981), 20

[10] M. Creutz; Phys. Rev. D21, (1980), 2308 and Phys. Rev. Lett. 45, (1980), 313

[11] E. Pietarinen; Nuc. Phys. B190, (1981), 349 and
N. Cabibbo and E. Marinari; Univ. of Rome Preprint No 301 (1982)

[12] H. Hamber and G. Parisi; Phys. Rev. Lett. 47, (1981), 1792
E. Marinari, G. Parisi and C. Rebbi; Phys. Rev. Lett., (1981), 1795
D. Weingarten; Phys. Lett. B109, (1982), 57

[13] R.C. Edgar in "Being discrete about Yang and Mills", PhD thesis, University College, London (1982)

[14] A.H. Guth; Phys. Rev. D21, (1980), 2291
J. Frolich and T. Spencer; Comm. Math. Phys. 83, (1982), 411

[15] T. Banks, J. Kogut and R. Myerson; Nuc. Phys. B129, (1977), 493

[16] M. Creutz, L. Jacobs and C. Rebbi; Phys. Rev. Lett. 42, (1979), 1390 and Phys. Rev. D20, (1979), 1915

[17] B. Lautrup and M. Nauenberg; Phys. Rev. Lett. 95B, (1980), 63

[18] K.J.M. Moriarty; Phys. Rev. D25, (1982), 2185 and J. Phys. G9, (1983), L33

[19] G. Bhanot; Phys. Rev. D24, (1981), 461

[20] D.G. Caldi; Nuc. Phys. B220 [FS8], (1983), 48

[21] J. Villain; J. Phys. C36, (1975), 581

[22] J.M. Kosterlitz and D.J. Thouless; J. Phys. C6, (1973), 118

[23] J.A. de Grand and D. Toussaint; Phys. Rev. D22, (1980), 2478

[24] J.L. Cardy; Nuc. Phys. B220 [FS1], (1980), 369

[25] J.M. Luck; Nuc. Phys. B170 [FS6], (1982), 330

[26] J.S. Barber; Phys. Lett. 147B, (1984), 330

[27] J.S. Barber, R. Shrader and R.E. Shrock; Phys. Lett. 152B, (1985), 221

[28] J. Jersak, T. Neuhaus and P.M. Zerwas; Phys. Lett. 133B, (1983), 103

[29] G. Bhanot; Nuc. Phys. B205, [FS5], (1982), 168

[30] D. Dagotto; Phys. Rev. D30, (1984), 1276

[31] H.G. Evertz, J. Jerzak, T. Neuhaus and P.M. Zerwas; Aachen preprint PITHA 84/09 (1984)

[32] P. Pfeuty and G. Toulouse in "Introduction to the Renormalization Group and Critical Phenomena", Chapt.12, Wiley, New York (1982)
I.D. Lawrie and S. Sarbach in "Phase Transitions and Critical Phenomena", Vol.9, (eds. C. Domb and J.L. Lebowitz), Academic Press, London (1984)

[33] D.P. Landau and R.H. Swendsen; Phys. Rev. Lett. 46, (1981), 1437

[34] K. Binder in "Monte Carlo Methods in Statistical Physics", Vol.5 (eds. C. Domb and M.S. Green), Academic Press, New York (1976)

[35] N. Metropolis, A.W. Rosenbluth, A.H. Teller and E. Teller; J. Chem. Phys. 21, (1953), 1087

[36] C.P. Yang; Proc. of Symposis in Applied Mathematics, Vol.XV, Amer. Math. Soc., Providence, RI, (1963), p.351

[37] J. von Neumann in "Monte-Carlo Methods", Nat. Bureau of Standards, Applied Mathematics series 12 (1951)

[38] C. Whitmer, Phys. Rev. D29, (1984), 306

[39] G.J. Daniell, A.J.G. Hey and J.E. Mandula; Phys. Rev. D30, (1984), 2230

[40] M.E. Fischer in "Proceedings of the International School of Physics Enrico Fermi" (Varenna, 1970) Course No.51, (ed. M.S. Green), Academic Press, New York (1971)

[41] K. Symanzik in "Mathematical problems in theoretical physics" (ed. R. Schroder), Lect. Notes in Physics 153, Springer (Berlin, 1982)

[42] C.J. Hamer and M.N. Barber; J.Phys. A13, (1980), L169
M.P. Nightingale, Physica A83, (1976), 561

[43] N.H. Christ, R. Friedberg and T.D. Lee; Nucl. Phys. B202, (1982), 89

[44] W. Celmaster; Phys. Rev. D26, (1982), 2955

[45] J.-M. Drouffe and K.J.M. Moriarty; Nucl. Phys. B220 [FS8], (1983), 253

[46] J.-M. Drouffe, K.J.M. Moriarty and C.N.-Mouhas; Comp. Phys. Comm. 30, (1983) 249

[47] A. Hasenfratz, E. Hasenfratz and P. Hasenfratz; Nucl. Phys. B181, (1981) 353
C.Itzyckson, M. Peskin and J.-B. Zuber; Phys. Lett. 95B, (1980), 259
M. Lüscher, G. Münster and P. Weisz; Nuc. Phys. B180, (1980), 1

[48] J.-M. Drouffe, K.J.M. Moriarty and C.N.-Mouhas; J. Phys. G10, (1984), 115

[49] K.G. Wilson and J. Kogut; Phys. Rep. C12, (1974), 75

[50] K.G. Wilson; Rev. Mod. Phys. 47, (1975) 773

[51] S.K. Ma; Phys. Rev. Lett. 37, (1976), 461

[52] R.H. Swendsen; Phys. Rev. Lett. 47, (1981), 1775

[53] R.H. Swendsen in "Monte-Carlo Renormalization Group Methods", Topics in Currrent Physics, Vol.30, p57 (eds. T.W. Burkhardt and J.M.J. van Leeuwen), Berlin, Spinger 1982

[54] G.S. Pawley, R.H. Swendsen, D.J. Wallace and K.J. Wilson; Edinburgh preprint 83/238

[55] R.H. Swendsen; Phys. Rev. Lett. 52, (1984), 1165

[56] A.N. Burkitt; Liverpool preprint LTH138 (1985)

[57] K.G. Wilson; Lecturer at Les Houches Summer School, France, 1980

[58] R. Gupta, M.A. Novotny and R. Cordery; NUB preprint (1985), 2654

[59] A.C. Irving and C.J. Hamer; Nucl. Phys. B235, (1984), 358